PLOS ONE

RESEARCH ARTICLE

Comparative genomics, infectivity and cytopathogenicity of Zika viruses produced by acutely and persistently infected human hematopoietic cell lines

Bingjie Li[1☯], Hsiao-Mei Liao[1☯], Hebing Liu[1], Shien Tsai[1], Jing Zhang[1], Guo-Chiuan Hung[1], Pei-Ju Chin[1], Yamei Gao[2], Shyh-Ching Lo[1]*

1 Tissue Microbiology Laboratory, Division of Cellular and Gene Therapies, Office of Tissues and Advanced Therapies, Center for Biologics Evaluation and Research, Food and Drug Administration, Silver Spring, Maryland, United States of America, **2** Lab of Pediatric and Respiratory Viral Diseases, Division of Viral Products, Office of Vaccines Research and Review, Center for Biologics Evaluation and Research, Food and Drug Administration, Silver Spring, Maryland, United States of America

☯ These authors contributed equally to this work.
* shyhching.lo@fda.hhs.gov

Citation: Li B, Liao H-M, Liu H, Tsai S, Zhang J, Hung G-C, et al. (2018) Comparative genomics, infectivity and cytopathogenicity of Zika viruses produced by acutely and persistently infected human hematopoietic cell lines. PLoS ONE 13(9): e0203331. https://doi.org/10.1371/journal.pone.0203331

Editor: Zheng Xing, University of Minnesota College of Veterinary Medicine, UNITED STATES

Received: May 1, 2018

Accepted: August 17, 2018

Published: September 7, 2018

Data Availability Statement: All relevant data are within the paper and its Supporting Information files. All reads mapping BAM files are available from the Dryad repository, doi: 10.5061/dryad.7r7812c.

Funding: This work was supported in part by the FDA Modernizing Science grant and FDA Zika supplement fund. The funders had no role in study design, data collection and interpretation or preparation of the manuscript for publication.

Abstract

Zika virus (ZIKV), an arthropod-borne virus, has emerged as a major human pathogen. Prolonged or persistent ZIKV infection of human cells and tissues may serve as a reservoir for the virus and present serious challenges to the safety of public health. Human hematopoietic cell lines with different developmental properties revealed differences in susceptibility and outcomes to ZIKV infection. In three separate studies involving the prototypic MR 766 ZIKV strain and the human monocytic leukemia U937 cell line, ZIKV initially developed only a low-grade infection at a slow rate. After continuous culture for several months, persistently ZIKV-infected cell lines were observed with most, if not all, cells testing positive for ZIKV antigen. The infected cultures produced ZIKV RNA (v-RNA) and infectious ZIKVs persistently ("persistent ZIKVs") with distinct infectivity and pathogenicity when tested using various kinds of host cells. When the genomes of ZIKVs from the three persistently infected cell lines were compared with the genome of the prototypic MR 766 ZIKV strain, distinct sets of mutations specific to each cell line were found. Significantly, all three "persistent ZIKVs" were capable of infecting fresh U937 cells with high efficiency at rapid rates, resulting in the development of a new set of persistently ZIKV-infected U937 cell lines. The genomes of ZIKVs from the new set of persistently ZIKV-infected U937 cell lines were further analyzed for their different mutations. The 2nd generation of persistent ZIKVs continued to possess most of the distinct sets of mutations specific to the respective 1st generation of persistent ZIKVs. We anticipate that the study will contribute to the understanding of the fundamental biology of adaptive mutations and selection during viral persistence. The persistently ZIKV-infected human cell lines that we developed will also be useful to investigate critical molecular pathways of ZIKV persistence and to study drugs or countermeasures against ZIKV infections and transmission.

Competing interests: The authors have declared that no competing interests exist.

Introduction

Transmission of ZIKV in French Polynesia and South America has been associated with the development of pathologic neurological symptoms and central nervous system abnormalities in the fetus [1–4]. Studies on the newly emerging infection of ZIKV have rapidly progressed on various fronts, including development of methods for rapid virus detection, medical treatments and vaccines against the Zika flavivirus [5–10]. Earlier studies revealed that ZIKV could be found in urine, semen, saliva or tears of infected patients long after the virus could no longer be detected in the patients' blood [11–14]. Long-term presence of v-RNA in body fluids is an indicator for prolonged or persistent viral infection in the body. However, cells that support continuous ZIKV replication and mechanisms by which the virus establishes persistence in various human tissues remain enigmatic.

Persistently flavivirus-infected cells hidden in tissues are often difficult to detect and may lead to devastating medical consequences. The incidents of transmitting fatal infection of West Nile Virus (WNV), another flavivirus, from WNV-infected organ donors who were no longer viremic during blood testing to recipients through organ transplantation are well-documented [15, 16]. To effectively prevent ZIKV transmission through transfusion of infected blood and particularly, through transplantation of infected organs or tissues, we need a better appreciation of the cells harboring the infectious virus and serving continuously as a ZIKV reservoir for a prolonged period of time. In addition, a better understanding of the key mechanisms of developing ZIKV persistence in these cells is needed.

An earlier study of acute experimental ZIKV infection in Rhesus Macaques revealed that the detection of v-RNA was more persistent in whole blood compared to plasma. Moreover, the study showed that many tissues contained v-RNA 14 days post-infection, when the infected animals were no longer viremia, with the highest levels in hemato-lymphatic tissues, such as lymph nodes and spleen [17]. Two other studies involving experimentally ZIKV-infected rhesus monkeys also reported that lymphoid tissues and central nervous system (CNS) cells had prolonged viral persistence [18, 19]. Thus, all three non-human primate studies of ZIKV infections demonstrated that the hemato-lymphatic system had the most prolonged infection [17–19]. Consistent with the study results of ZIKV-infected monkeys, the study of patients who had benign ZIKV infections similarly revealed that ZIKV v-RNA persisted in whole blood samples substantially longer than in plasma [20]. Taken together, these findings suggested the presence of yet-to-define cells allowing prolonged or persistent ZIKV infection in the hemato-lymphatic tissues and blood of the ZIKV-infected experimental monkeys as well as patients.

To investigate possible ZIKV persistence in cells of hemato-lymphatic system and blood, we examined the relative susceptibility of human hematopoietic cell lines with different developmental characteristics to infection of the prototype MR 766 ZIKV strain and focused on the duration as well as the outcome(s) of the infection. Significantly, we found that human monocytic leukemia/histiocytic lymphoma-originated U937 cell line [21], initially showing a slow rate and low grade infection using ZIKV MR 766 strain, could develop into persistently ZIKV-infected cell lines in which most of the cells in the culture were positive for ZIKV antigens despite no apparent cytopathological changes. We measured the amounts of v-RNA genomes and compared the titers of infectious ZIKV virions produced by persistently ZIKV-infected U937 cells growing as continuous cultures established in the context of 3 separate experiments. We first compared the "persistent ZIKVs" produced by the 3 persistently ZIKV-infected cell lines with the inoculum prototype strain MR 766 ZIKV for their infectivity and pathogenicity against human hematopoietic cells with different developmental characteristics. Furthermore, we conducted a detailed comparative genome sequence analyses among 1) the inoculum prototype strain MR 766 ZIKV, 2) the "early phase ZIKVs" produced by U937 cells infected by

MR 766 ZIKV in the first 1–2 weeks, 3) the "persistent ZIKVs" (1st generation) produced by the 3 continuous U937 cell lines that developed viral persistence following infections of prototype strain MR 766 ZIKV, and 4) the "persistent ZIKVs" (2nd generation) produced by the 3 continuous U937 cell lines that developed viral persistence following infections with the 3 respective 1st generation persistent ZIKVs. The apparent dynamic interplay between ZIKVs and the infected host cells to confer viral persistence following each viral infection is discussed.

Results

Susceptibility of immortalized human hematopoietic cells with different developmental characteristics to ZIKV infection

A number of human B cell lines, T cell lines and myelogenous/monocytic cell lines (see Table 1) were infected by ZIKV at MOI of 2 for 2 hours, washed twice using PBS and re-suspended in fresh culture media. The effectiveness and efficiency of ZIKV infection in the cultured human hematopoietic cells were monitored by the kinetics of cells becoming positive for ZIKV-specific antigens using an immunofluorescent assay (IFA) and developing virus infection associated cytopathological effect (CPE) changes with cytolytic necrosis. Cells of non-ZIKV-infected control cultures were studied in parallel for comparison.

Table 1 summarizes the study results showing that all five examined B lymphoblastoid cell lines were highly susceptible to ZIKV infection, turning positive for ZIKV antigens in IFA within the first few days. These B lymphoblastoid cell lines also developed prominent CPE changes with cell necrosis or cytolysis in the cultures observed within a week following ZIKV infection. ZIKV v-RNA genomes ($>10^8$ copies/ml) were found in the culture supernatants of these human B cell lines. In contrast, T lymphoblastoid cell lines appeared to be very resistant

Table 1. Human hematopoietic cells with different developmental characteristics showed different susceptibility to ZIKV (strain MR 766) infection.

Name of human cell line	Cell type	Susceptibility to infection*	Viral CPE observed**	v-RNA genome copies/ml (Day 6)
B cell lines				
CCRF-SB	B lymphoblastoid cells	Susceptible	Y	1.60×10^8
RPMI 8392	B lymphoblastoid cells	Susceptible	Y	1.52×10^8
K2267-Mi	B lymphoblastoid cells	Susceptible	Y	2.18×10^8
824–00	B lymphoblastoid cells	Susceptible	Y	8.07×10^8
4695EB	B lymphoblastoid cells	Susceptible	Y	2.60×10^9
T cell lines				
CCRF-CEM	T lymphoblastoid cells	Resistant	N	NA
CCRF-HSB2	T lymphoblastoid cells	Resistant	N	NA
Molt-3	T lymphoblastoid cells	Resistant	N	NA
RPMI 8402	T lymphoblastoid cells	Resistant	N	NA
Myelogenous Monocytic cell lines				
K562 (K)	Chronic myelogenous leukemia	Susceptible	Y	1.02×10^{10}
U937 (U)	Histiocytic lymphoma	Susceptible#	N	2.19×10^7
THP-1	Monocytic leukemia	Resistant	N	NA
HL-60	Promyelocytic leukemia	Resistant	N	NA
KG-1	Myelocytic leukemia	Resistant	N	NA

*__Susceptibility to infection:__ Finding ZIKV-specific antigen positive cells by immunofluorescent staining within a week of ZIKV infection in the culture.

__#Susceptible:__ ZIKV-specific antigen positive cells could be found in the culture, but only at low numbers.

**__CPE observed:__ Cells showing cytopathological changes and cytolytic necrosis that resulted in significantly lower numbers (<50%) of viable cells found in the ZIKV-infected cultures in comparison with those in the non-ZIKV-infected control cultures.

https://doi.org/10.1371/journal.pone.0203331.t001

to the infection of ZIKV. None of the four T lymphoblastoid cell lines turned positive for ZIKV-specific antigens in IFA or developed detectable CPE changes following more than 1 week of ZIKV infection in the cultures. The study revealed ZIKV infectivity of human myelogenous/monocytic cell lines varied. The three myelogenous cell lines, THP-1, HL-60 and KG-1, were resistant to the ZIKV infection without having turned into ZIKV-specific antigens positive cells or having developed CPE changes with cell necrosis in the infected cultures. However, the prototype MR 766 ZIKV strain could infect 2 of the human myeloid cell lines, K562 and U937. Fig 1 provides a schematic diagram that depicts the workflow of studying ZIKV infections in different human hematopoietic cell lines and the process of establishing persistently ZIKV-infected human monocytic/histiocytic U937 cell lines.

Prototype strain MR 766 ZIKV infected myelogenous K562 cell line and monocytic/histiocytic U937 cell line at different rates with different efficiencies

The human cell line K562 that originated from myelogenous leukemia was highly susceptible to ZIKV infection. Specifically, more than 70% of myelogenous K562 cells were already turning positive for immunofluorescent staining of ZIKV antigens in the culture 3 days post ZIKV infection. Many K562 cells had prominent CPE changes and underwent cytolytic necrosis resulting in significantly lower number (~30%) of viable cells than that in the non-infected control culture at day 4. A large amount of ZIKV v-RNA genomes (up to 10^{10} copies/ml) were found in the culture supernatant (Table 1). In comparison, the monocytic

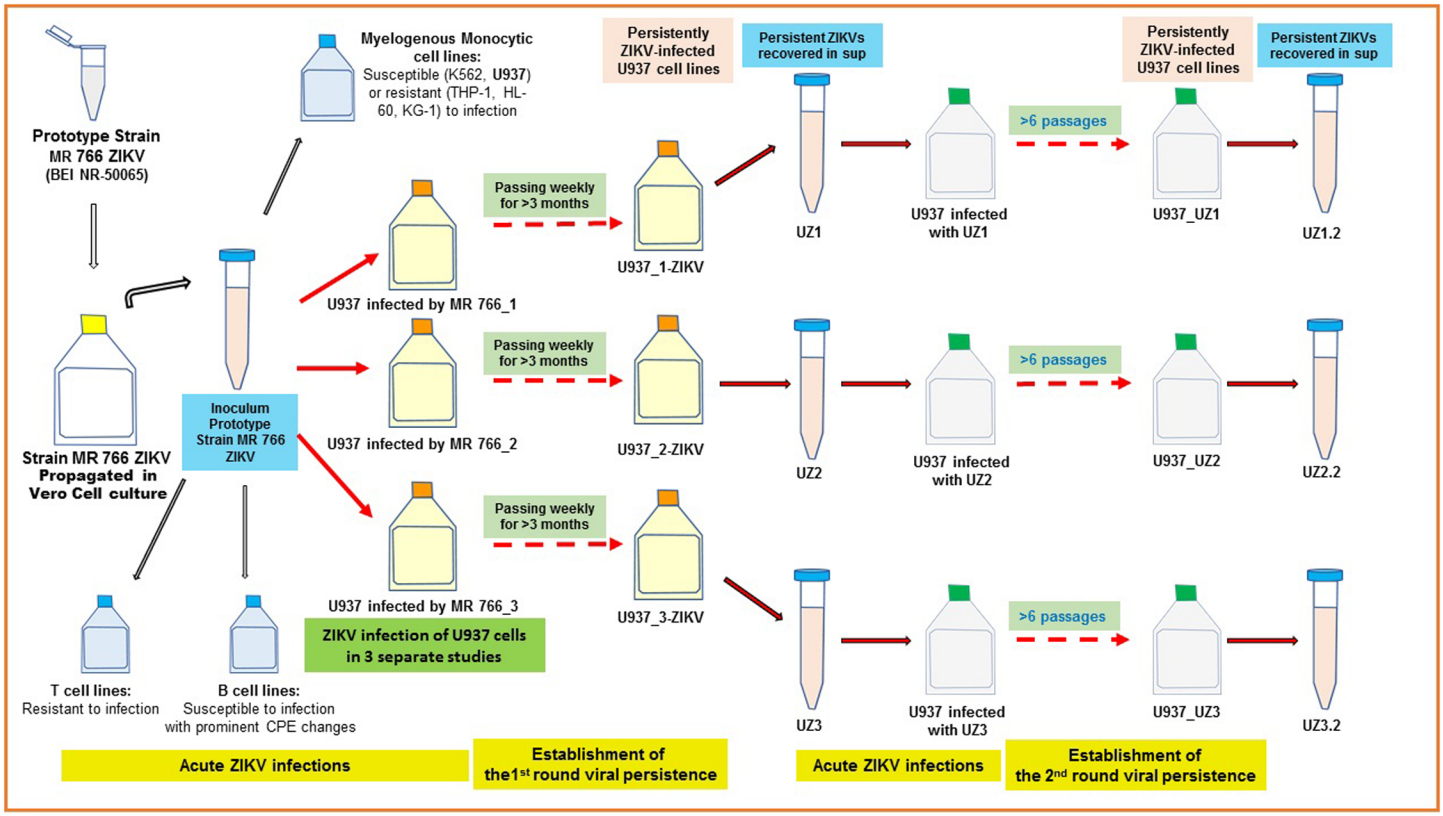

Fig 1. The schematic illustration of the experimental workflow and the establishment of persistently ZIKV-infected U937 cell lines.

https://doi.org/10.1371/journal.pone.0203331.g001

leukemia/histiocytic lymphoma-originated U937 cells were much less susceptible to ZIKV infection. Fig 2A shows consistent slow rates and low grade of ZIKV infections in the U937 cell cultures infected with the prototype strain MR 766 ZIKV in 3 separate studies (U937-MR 766_1, U937-MR 766_2 and U937-MR 766_3). Only small numbers of cells tested IFA-positive for ZIKV specific antigen in the cultures following 1–2 weeks of ZIKV infections (Fig 2B). Moreover, the prominent CPE changes and cell loss seen in the ZIKV-infected culture of myelogenous K562 cells could not be detected in the monocytic/histiocytic cultures of U937 cells with the low grade ZIKV infection. In all 3 experiments involving U937 cells, the numbers of viable U937 cells found daily in the ZIKV-infected cultures and the non-infected control cultures were essentially the same.

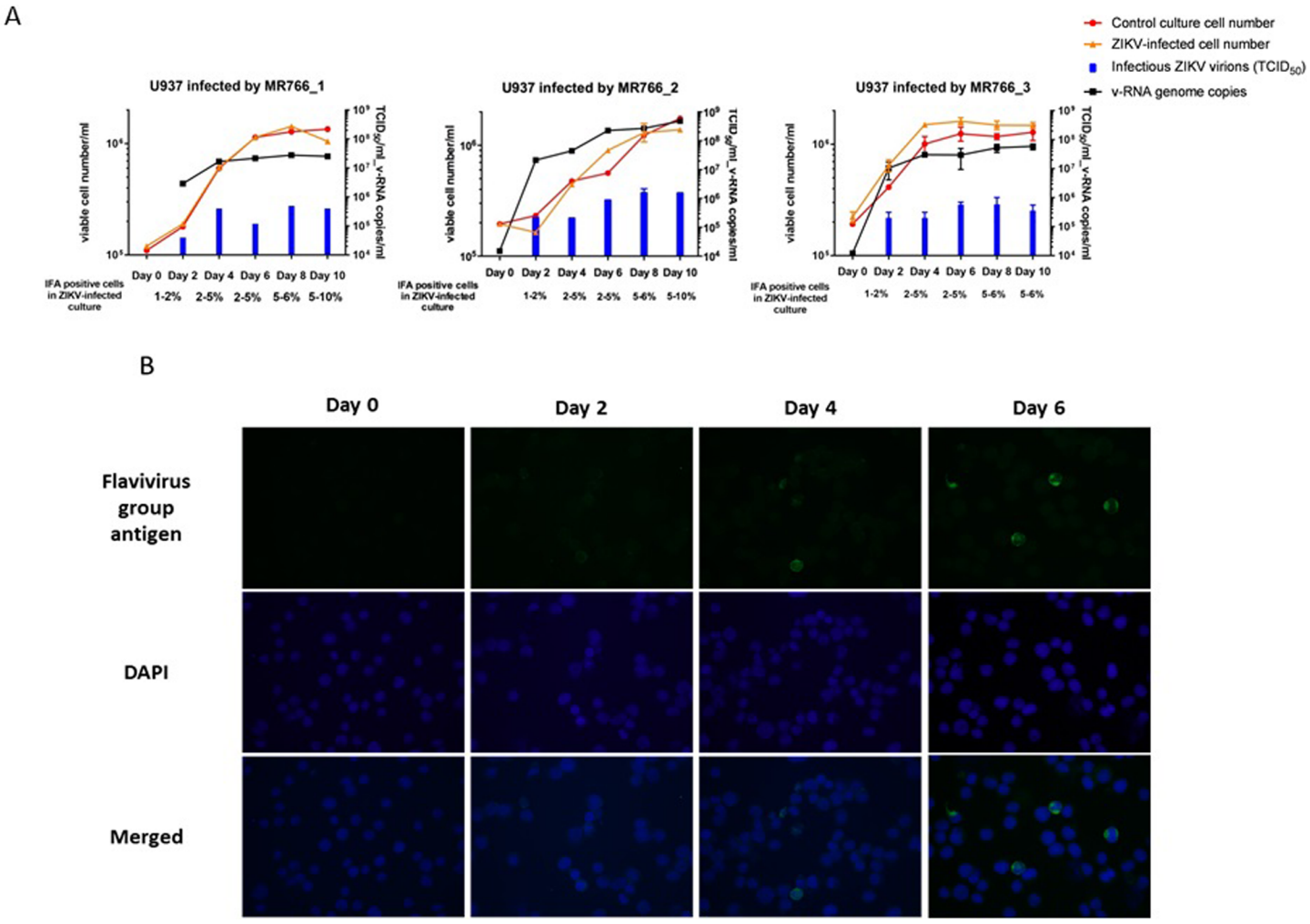

Fig 2. (A) Cell growth, numbers of cells turning IFA-positive for ZIKV antigen, production of ZIKV RNA genomes and infectious virions in U937 cell cultures with and without infection of Prototype ZIKV Strain MR 766 in 3 separate studies. Viable cells were determined by trypan blue dye exclusion. Quantitation of v-RNA ZIKV genomes by RT-PCR and titration of infectious ZIKV virions by $TCID_{50}$ assay were examined in the supernatants of U937 cell cultures every 2 days. No ZIKV v-RNA and no infectious ZIKV virion could be detected in supernatants of the 3 non-ZIKV infected control U937 cell cultures. **(B) IFA of cells positively producing ZIKV-specific antigens in U937 cell culture infected with ZIKV Strain MR 766 in the early phase.** Anti-flavivirus group antigen monoclonal antibody was used as the primary IFA antibody for staining day 0 to day 6 cells in the U937-MR 766_1 culture. Merged: the merged image stacks the immunofluorescent staining of flavivirus group antigen and DAPI nuclear staining of cells.

https://doi.org/10.1371/journal.pone.0203331.g002

Development of persistently ZIKV-infected U937 cell lines

Although ZIKV infection in the U937 cell cultures had only small numbers of ZIKV antigen positive cells and essentially no cells dying of viral infection-associated CPE in the first 1–2 weeks, both ZIKV v-RNA genomes (~4×10^7 copies/ml) and infectious virions (~5×10^5 ID_{50} units/ml) could be detected in supernatants of the 3 ZIKV-infected cultures (Fig 2A). Noticeably, increasing numbers of U937 cells were becoming IFA-positive for ZIKV antigen in the cultures that were diluted and replenished weekly with fresh medium to support continued growth of the viable cells in cultures. By continuously passing U937 cells that were growing in the MR 766 strain ZIKV-infected cultures established separately in the 3 studies U937-MR766_1, U937-MR766_2 and U937-MR766_3 for more than 3 months, we found most, if not all, cells in the 3 cultures tested positive for ZIKV-specific antigen (Fig 3). The continuous U937 cell lines

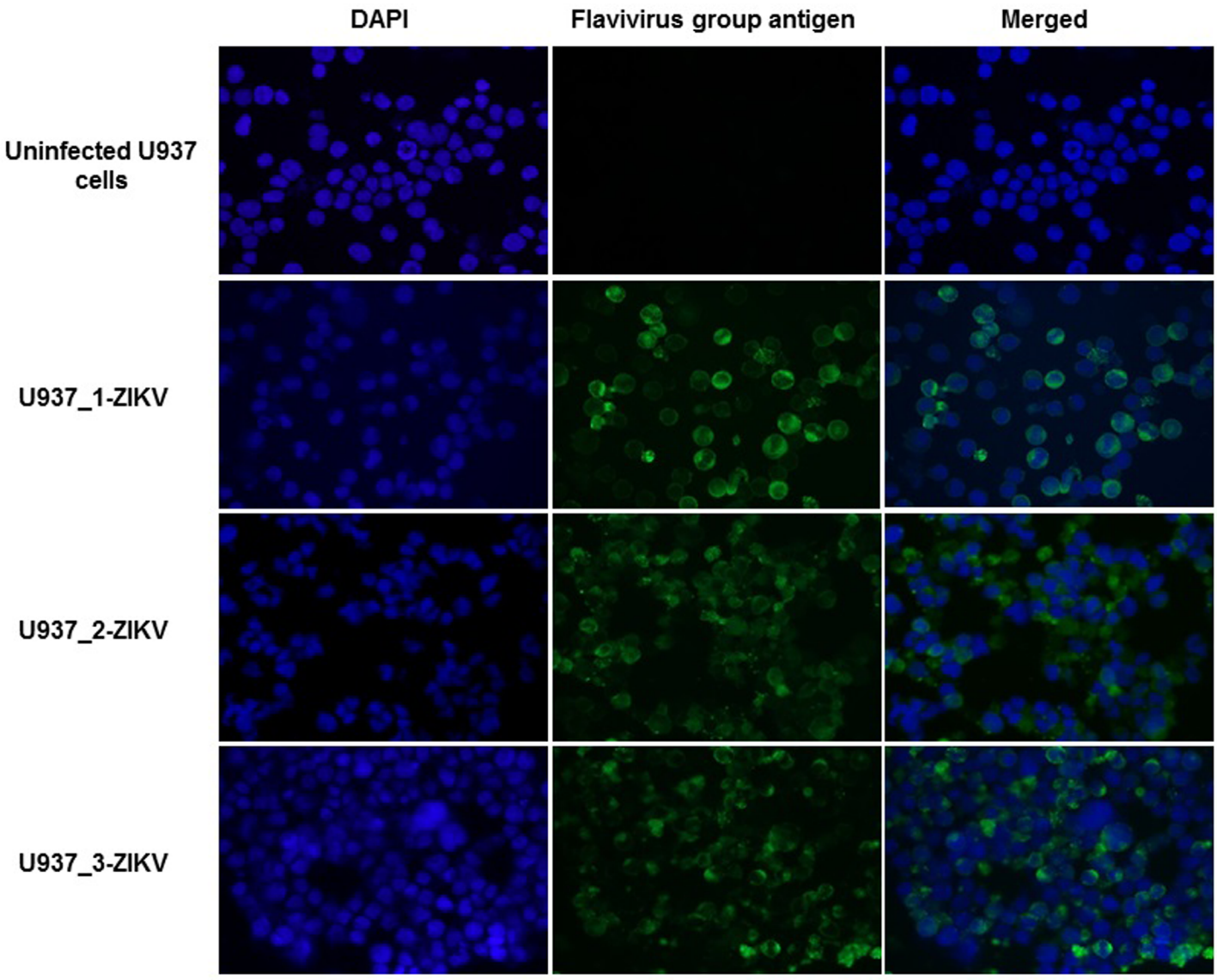

Fig 3. IFA of ZIKV antigen-positive cells in the U937 cell cultures continuously passed for more than 2 months following infections of Prototype ZIKV Strain MR 766. The 3 continuous U937 cell lines U937_1-ZIKV (A), U937_2-ZIKV (B) and U937_3-ZIKV (C) appeared to be persistently infected with ZIKV. Most of cells in the 3 cultures were positively stained for ZIKV specific antigen. Merged: the merged image stacks the immunofluorescent staining of flavivirus group antigen and DAPI nuclear staining of cells.

https://doi.org/10.1371/journal.pone.0203331.g003

with apparent persistent ZIKV infection established from the 3 separate experiments were designated as U937_1-ZIKV, U937_2-ZIKV and U937_3-ZIKV, respectively (Fig 1). Transmission electron microscopy (TEM) examination of the persistently ZIKV-infected U937 cells revealed large numbers of electron-dense particles with size of ~35 nm in the cytoplasm. Although some of these "virus-like" particles were found in the vesicles, most of them appeared to be free of association with any subcellular structures in the cytoplasm. The nature of these particles in the cytoplasm needs further investigations (**S1 Fig**).

ZIKV v-RNA genomes and infectious virions produced by the persistently ZIKV-infected U937 cell lines

We measured both ZIKV v-RNA genomes and infectious virions produced by U937 cells after establishment of persistent ZIKV infection in the 3 ZIKV-infected cultures. In this study, U937 cells in suspension of each persistently ZIKV-infected culture were harvested by centrifugation and re-suspended in fresh media every 2 days. We quantitatively measured both the copy numbers of ZIKV v-RNA genome by RT-PCR and the titers of ZIKV virions that were capable of infecting Vero cells ($TCID_{50}$ units), released into the culture supernatants in 2 days (Fig 4). Panel A graph in Fig 4 shows that ~4×10^8 copies/ml of ZIKV genome RNA and ~3×10^6 ID_{50} units/ml of infectious ZIKV virions were consistently produced and released into culture supernatants by 0.5–1×10^6 cells/ml of the cultured U937_1-ZIKV cell line in 2 days. The ratios between copy numbers of ZIKV v-RNA genome and titers of infectious virions in the culture supernatants were ~100-fold.

Panel B graph in Fig 4 shows that ~6×10^7 copies/ml of ZIKV v-RNA genome were produced and released into culture supernatants by 0.5–1×10^6 cells/ml of the cultured U937_2-ZIKV cell line in 2 days. However, infectious of ZIKV virions could not be documented in the culture supernatants using the standard $TCID_{50}$ assay. No typical CPE changes with associated cytolytic necrosis and cell sloughing off in the wells were detected in the $TCID_{50}$ assay conducted on Vero cells. However, occasional foci of cell aggregates with atypical CPE were seen in the wells seeded with Vero cells and inoculated with low dilution ($\leq10^2$) of the supernatants obtained from the culture of U937_2-ZIKV cell line (S2 Fig). The U937_2-ZIKV culture could be producing $\leq10^2$ ID_{50} unit/ml of infectious ZIKV virions in the supernatant, if the atypical CPE without cytolytic necrosis or cell sloughing was considered as positive of ZIKV infection in the $TCID_{50}$ assay against cultured Vero cells, The ratios between copy numbers of ZIKV v-RNA genome and titers of infectious ZIKV virions found in the culture supernatants appeared to be extremely high (near 10^6 fold). Panel C graph in Fig 4 shows that ~6×10^8 copies/ml of ZIKV v-RNA genomes and 6–8×10^5 ID_{50} units/ml of infectious virions were consistently produced and released into culture supernatants by 0.5–1×10^6 cells/ml of the cultured U937_3-ZIKV cell line in 2 days (Fig 4C). The ratios between copy numbers of ZIKV v-RNA genome and titers of infectious ZIKV virions found in the culture supernatants were ~1000-fold.

Susceptibility of human hematopoietic cells with different developmental characteristics to infections of ZIKVs produced by the persistently ZIKV-infected U937 cell lines

We examined the cell infection specificity, efficiency and pathogenicity of the ZIKVs produced by the U937 cell lines after establishment of ZIKV persistence in comparison with those of the prototype MR 766 strain ZIKV. Like the prototype ZIKV Strain MR 766, the "persistent ZIKVs" (UZ1, UZ2 and UZ3) produced in the 3 cultures of persistently ZIKV-infected U937 cell lines (U937_1-ZIKV, U937_2-ZIKV and U937_3-ZIKV, Fig 1) could not infect the examined human T cell lines (Table 2). However, the 3 "persistent ZIKVs" also could not infect the

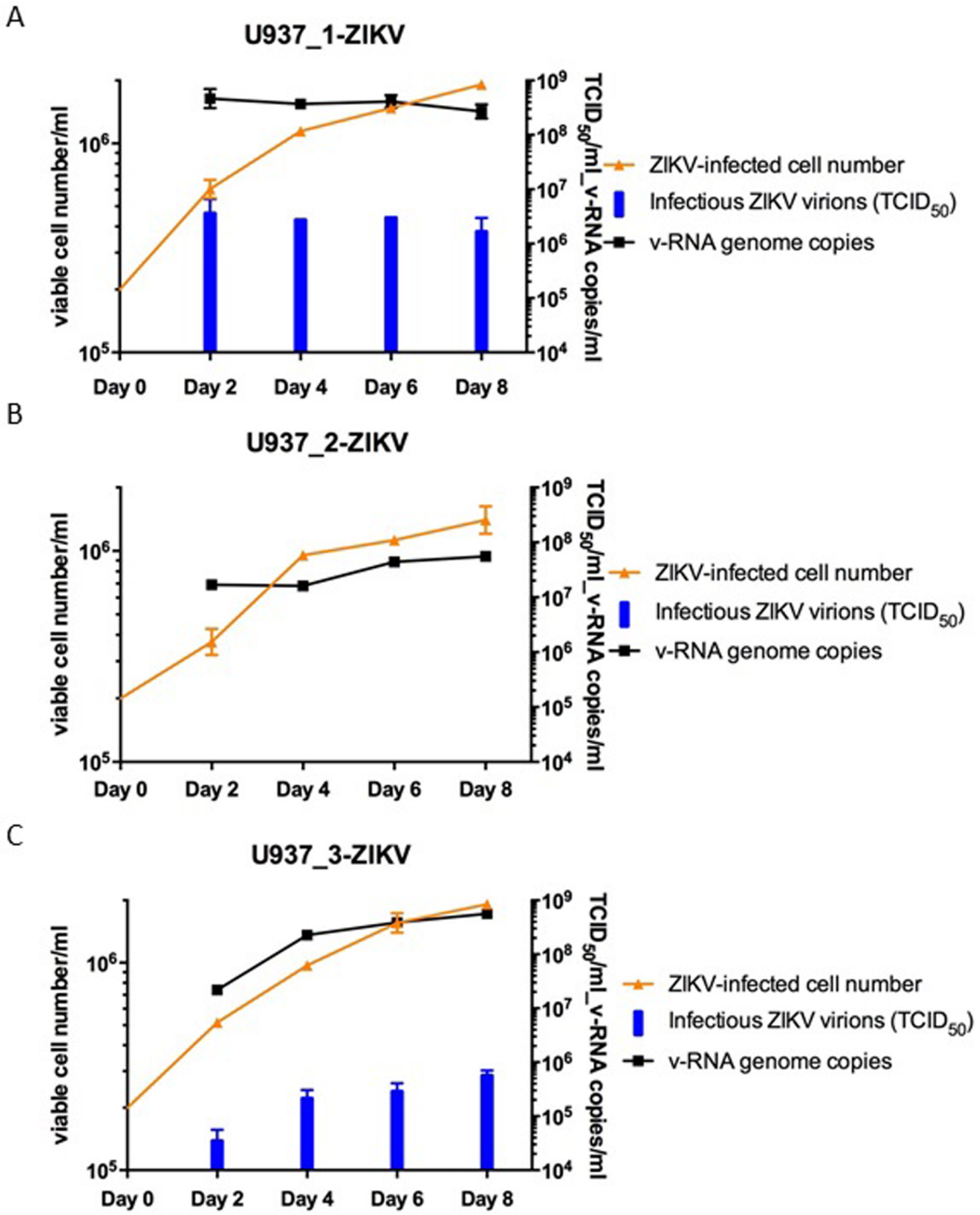

Fig 4. Cell growth, productions of ZIKV RNA genomes and infectious virions in cultures of the 3 continuous U937 cell lines that developed into viral persistence following Prototype ZIKV Strain MR 766 infection. Cells in the persistently ZIKV-infected cultures U937_1-ZIKV (A), U937_2-ZIKV (B) and U937_3-ZIKV (C), were harvested by centrifugation and re-suspended in fresh culture media every 2 days. The amounts of ZIKV RNA genomes and infectious virions produced into supernatants of the cultures in 2 days were quantified by qPCR and titrated by $TCID_{50}$ assay against Vero cells.

https://doi.org/10.1371/journal.pone.0203331.g004

human B cell lines CCRF-SB and RPMI8392 that were susceptible to infection by the prototype strain MR 766 ZIKV. Moreover, although the persistent ZIKVs UZ1 and UZ3 could infect

Table 2. Susceptibility of human hematopoietic cell lines to infection of ZIKV MR 766 and the persistent ZIKVs UZ1, UZ2 and UZ3.

Inoculated ZIKV	None		MR 766		UZ1		UZ2		UZ3	
v-RNA genome copy number of inoculation	None		2×10^8		2×10^8		2×10^8		2×10^8	
IFA Observation	Day 5	Day 7	Day 5	Day 7	Day 5	Day 7	Day 5	Day 7	Day 5	Day 7
B cell lines										
CCRF-SB	N	N	>30%+	70% +, CPE	N	N	N	N	N	N
RPMI 8392	N	N	100%+, CPE	100% +, CPE	N	N	N	N	N	N
K2267-Mi	N	N	10%+	100% +, CPE	~10%+	100% +	N	N	10%+	50%+
824–00	N	N	>30%+	100% +, CPE	>90%+	100% +	N	N	50%+	99%+
4695EB	N	N	100%+, CPE	100% +, CPE	>90%+	100% +	N	N	70%+	100%+
T cell lines										
CCRF-CEM	N	N	N	N	N	N	N	N	N	N
CCRF-HSB2	N	N	N	N	N	N	N	N	N	N
Molt-3	N	N	N	N	N	N	N	N	N	N
RPMI 8402	N	N	N	N	N	N	N	N	N	N
Myelogenous Monocytic cell lines										
K562 (K)	N	N	>90%+, CPE*	100% +, CPE*	100%+, CPE*	100%+, CPE*	100%+, CPE*	100% +, CPE*	100%+, CPE*	100%+, CPE*
U937 (U)	N	N	1–2%+	2–5% +	100%+, CPE*	100%+, CPE*	100%+, CPE*	100% +, CPE*	100%+, CPE*	100%+, CPE*
THP-1	N	N	N	N	N	N	N	N	N	N
HL-60	N	N	N	N	N	N	N	N	N	N
KG-1	N	N	N	N	N	N	N	N	N	N

All testing cultures were set up under 10 ml volume with 2×10^5 cells/ml. The testing cultures were inoculated with the supernatants prepared from cultures of the prototype ZIKV MR 766-infected Vero cells or the persistently ZIKV-infected U937 cells (U937_UZ1, U937_UZ2 and U937_UZ3) at MOI of 1 for ZIKV MR 766 (with 2×10^7 MR 766 v-RNA genome copies/ml) or with the same amount of ZIKV v-RNA genomes for UZ1, UZ2 and UZ3.

The percentage of IFA positive cells was estimated under fluorescent microscope at 200x and 400x.

CPE*: CPE with extensive cytolytic changes and cell death.

https://doi.org/10.1371/journal.pone.0203331.t002

human B cell lines K2267-Mi, 824–00 and 4695EB and effectively turn them IFA-positive for ZIKV-specific antigen, they did not produce prominent CPE changes with associated cytolytic necrosis found in the strain MR 766 ZIKV-infected cultures of these B cell lines (Table 2). The study further revealed that the persistent ZIKV UZ2 that exhibited very low infectivity and cyto- pathogenicity in the $TCID_{50}$ assay against Vero cells (Fig 4, graph B) could not infect any of the 5 human B cell lines that were highly susceptible to infection by the prototype strain MR 766 ZIKV. However, like the prototype strain MR 766 ZIKV, all 3 persistent ZIKVs, UZ1, UZ2 and UZ3, could effectively infect human myeloid hematopoietic K562 cells (Table 2). Nearly all K562 cells in the cultures infected by the 3 persistent ZIKVs became IFA-positive for ZIKV antigen in less than a week. The K562 cells in the infected-cultures showed prominent CPE changes and had extensive cytolytic necrosis (**S3 Fig**). Hence, it was difficult to maintain continued growth of the remaining viable K562 cells in the cultures infected by the 3 persistent ZIKVs after a week. Like the persistent ZIKV UZ2, ZIKV virions released in the culture of UZ2-infected K562 cell exhibited no infectivity with clear cytolytic necrosis and cell sloughing in the $TCID_{50}$ assay using Vero cells (Panel B graph in S3 Fig).

In contrast to the prototype strain MR 766 ZIKV; all 3 established "persistent ZIKVs" could rapidly infect fresh U937 cells in culture with high efficiency (Table 2). Fig 5 shows that more than 90% of U937 cells were positive for ZIKV antigen in the cultures of infected by each persistent ZIKVs at day 4, when <5% of U937 cells in the cultures infected by prototype MR 766 ZIKV strain tested positive (Fig 2). Furthermore, infections of the 3 persistent ZIKVs in the U937 cell cultures produced prominent CPE changes with cytolytic necrosis, not observed in the U937 cell cultures infected by the prototype strain MR 766 ZIKV. The number of viable cells in the U937 cell cultures infected by each of the 3 persistent ZIKVs after a week were significantly lower (<20%) than that in the non-infected control culture (Fig 5). The persistent ZIKV UZ2 that did not effectively infect Vero cells and all the human B cell lines appeared to be the most cytopathogenic ZIKV that produced the most serious CPE and cytolytic necrosis in the infected U937 cells culture (Panel B graph in Fig 5). Like the persistent ZIKV UZ2, ZIKV virions produced in the culture of UZ2-infected U937 cells showed no clear infectivity with detectable cytolytic necrosis in the $TCID_{50}$ assay using Vero cells.

Establishing a 2nd generation of persistently ZIKV-infected U937 cell lines from fresh U937 cell cultures infected with the 1st generation persistent ZIKVs

The small numbers of viable U937 cells began to re-grow in the UZ1 and UZ3-infected cultures after 2 weeks. An even smaller number of viable U937 cells in the UZ2-infected culture also recovered and began to re-grow after 3 weeks. By further passing the U937 cells that were growing in the cultures infected by the respective 3 persistent ZIKVs for more than 2 months (more than 6 passages), we established 3 continuous U937 cell lines with most, if not all, of the growing cells in the cultures being IFA-positive for ZIKV-specific antigen (Fig 6). These U937 cell lines with apparent persistent ZIKV infection (the 2nd generation) established by infecting fresh U937 cells in culture with the 3-pre-established persistent ZIKVs UZ1, UZ2 and UZ3 were designated as U937_UZ1, U937_UZ2 and U937_UZ3, respectively (Fig 1).

Fig 7 (panel graphs A and C) shows that ~10^9 copies/ml of ZIKV v-RNA genomes and ~3×10^6 ID_{50} units/ml of infectious ZIKV virions were produced by $0.5–1\times10^6$ cells/ml of cultured U937_UZ1 and U937_UZ3 cell lines every 2 days. In comparison, $1–2\times10^8$ copies/ml of ZIKV v-RNA genome were also produced by $0.5–0.8\times10^6$ cells/ml of cultured U937_UZ2 cell line every 2 days. However, no infectious ZIKV virions that could produce typical CPE with cytolytic necrosis in the $TCID_{50}$ study conducted on seeded Vero cells (Panel graph B in Fig 7). The cell specificity for infectivity and pathogenicity of the 2nd generation persistent ZIKVs, UZ1.2, UZ2.2 and UZ3.2, produced by the cultures of U937_UZ1, U937_UZ2 and U937_UZ3 cell lines was the same as those of the respective 1st generation persistent ZIKVs, UZ1, UZ2 and UZ3. Specifically, like the 1st generation persistent ZIKV UZ2, the 2nd generation persistent ZIKV UZ2.2 also showed no typical CPE with cytolytic necrosis on Vero cells in $TCID_{50}$ assay (Fig 7, panel graph B) and no infectivity against the 5 human B cell lines referred to in Table 2. However, like UZ2, UZ2.2 infected K562 cells and U937 cells effectively. UZ2.2 produced prominent CPE changes with extensive cell necrosis in the infected cultures (data not shown).

Comparative genomics of the inoculum prototype strain MR 766 ZIKV and ZIKVs produced by acutely MR 766 ZIKV-infected U937 cells with the reported MR 766 reference genome sequence

RNA was recovered from **1)** the prototype ZIKV MR 766 viral stock provided by BEI Resources, **2)** the supernatants of the Vero cells cultures used to propagate BEI-derived MR 766 viral stocks

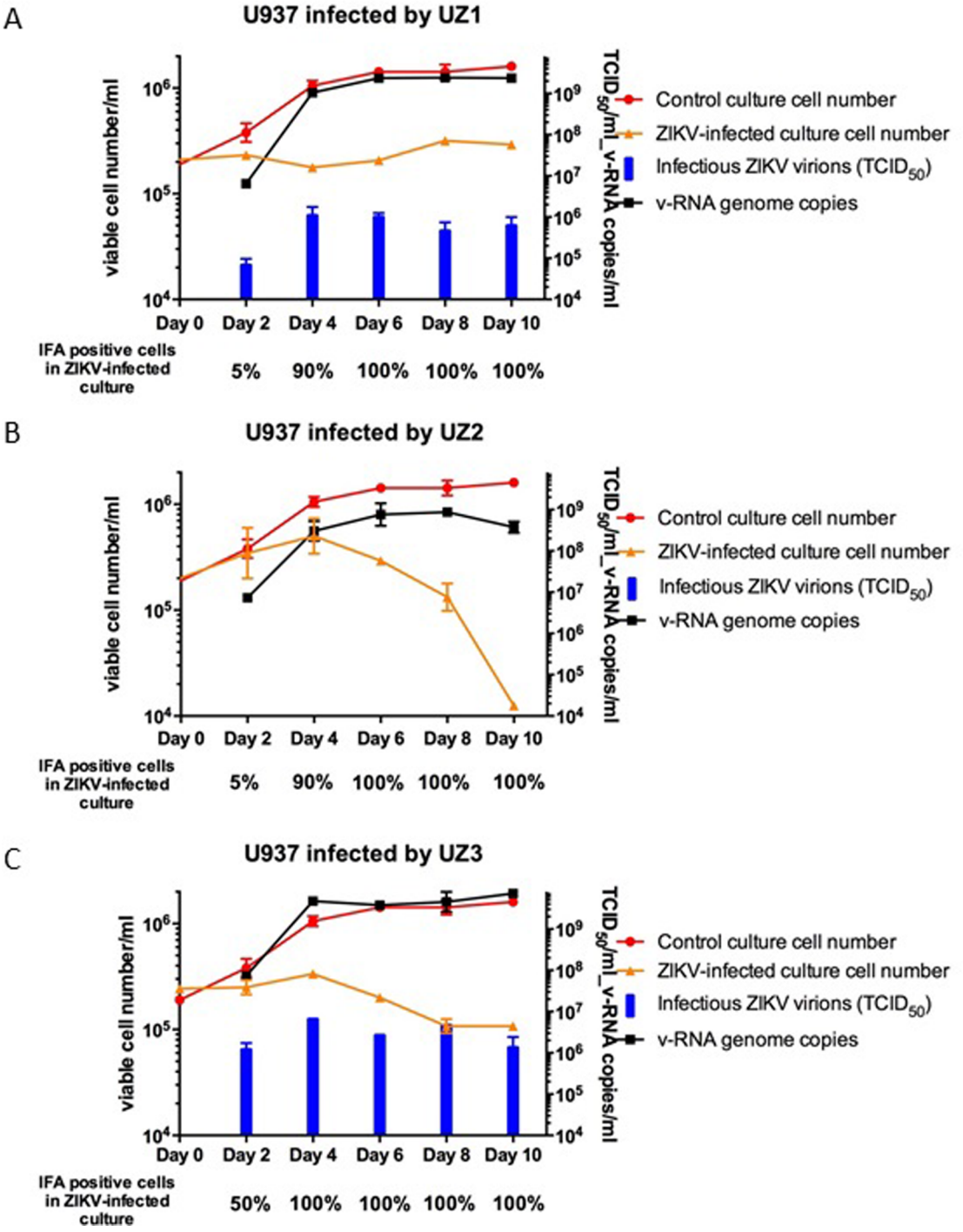

Fig 5. Cell growth, numbers of cells IFA-positive for ZIKV antigen, productions of ZIKV RNA genomes and infectious virions in cultures of fresh U937 cells infected with the 3 persistent ZIKVs UZ1(A), UZ2 (B) and UZ3 (C). The cultures of fresh U937 cells (2×10^5 cells/ml) were infected with the 3 persistent ZIKVs (~10^7 copies of ZIKV v-RNA genome/ml) prepared from the culture supernatants of persistently ZIKV-infected U937 cell lines U937_1-ZIKV, U937_2-ZIKV and U937_3-ZIKV. Prominent CPE with extensive cytolysis and cell loss were seen in all the 3 cultures infected with the 3 persistent ZIKVs UZ1, UZ2 and UZ3. The amounts of ZIKV RNA genomes and infectious virions produced into supernatants of the ZIKV-infected cultures were quantified by qPCR and titrated by $TCID_{50}$ assay against Vero cells.

https://doi.org/10.1371/journal.pone.0203331.g005

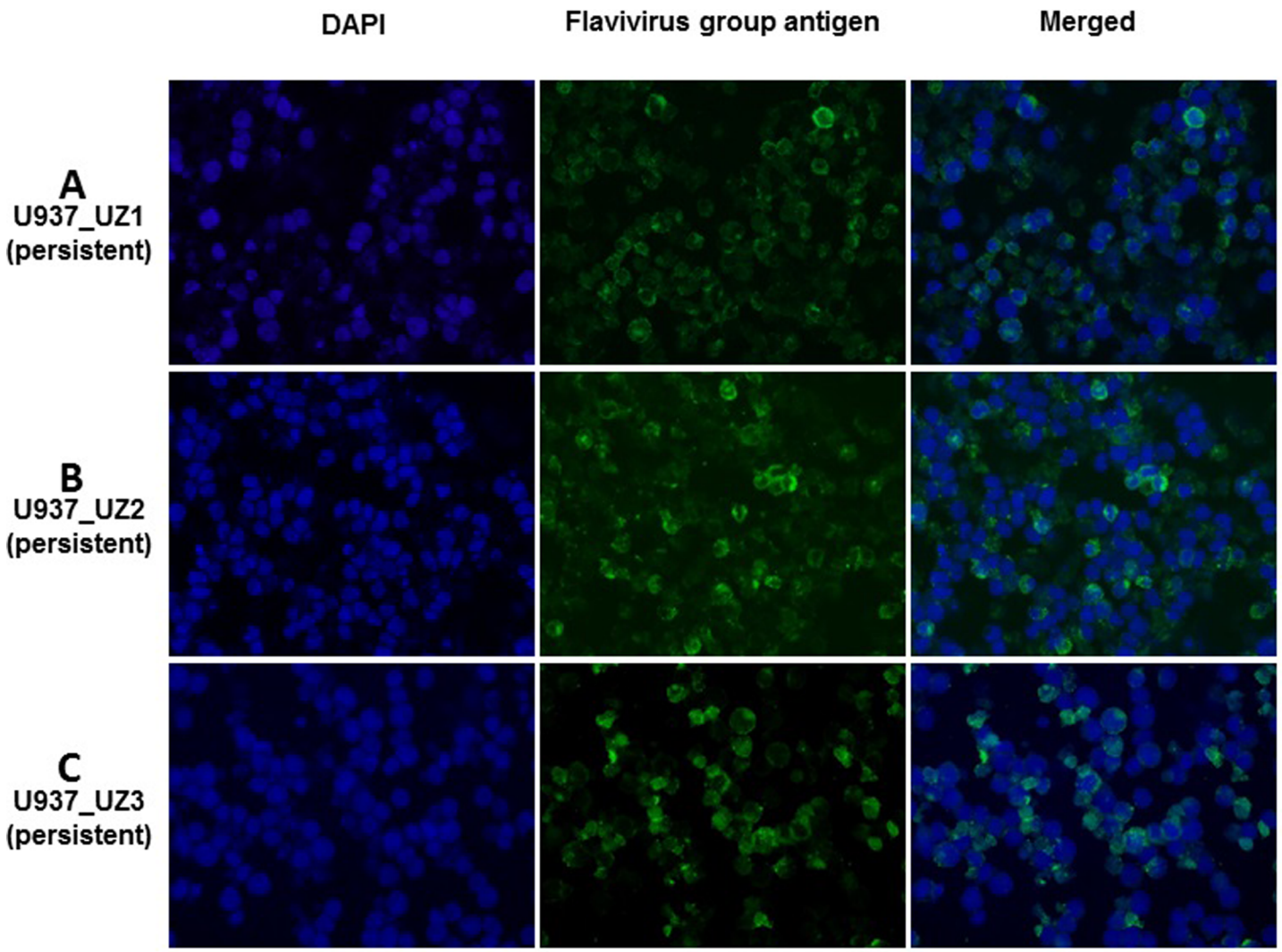

Fig 6. IFA of ZIKV antigen-positive cells in the 3 continuous U937 cell lines established from continuously passing the viable cells that recovered from U937 cell cultures infected with the 3 persistent ZIKVs UZ1, UZ2 and UZ3. The 3 continuous U937 cell lines were persistently infected with ZIKV and designated as (A) U937_UZ1 (persistent), (B) U937_UZ2 (persistent) and (C) U937_UZ3 (persistent), respectively. Merged: the merged image stacks the immunofluorescent staining of flavivirus group antigen and DAPI nuclear staining of cells.

https://doi.org/10.1371/journal.pone.0203331.g006

(MR 766/Vero) to be used as the inoculums for the present study and **3)** the supernatants of the U937 cell cultures infected by MR 766 ZIKV or the persistent ZIKVs UZ1 and UZ2 for the first 1–2 weeks (early phase). Furthermore, RNA was similarly recovered from **1)** the supernatants of the 3 cultures of persistently ZIKV-infected U937 cells (U937_1-ZIKV, U937_2-ZIKV and U937_3-ZIKV) established from the cultures infected by ZIKV Strain MR 766 and **2)** the supernatants of the 3 cultures of persistently ZIKV-infected U937 cells (U937_UZ1, U937_UZ2 and U937_UZ3) established from cultures infected by the persistent ZIKVs UZ1, UZ2 and UZ3, respectively (Fig 1). The RNAs were processed for v-RNA genomic sequencing using the MiSeq platform. The variations or mutations of nucleotide sequences different from the reference ZIKV strain MR 766 genome sequence [22] were identified. Nucleotide variations or mutations with less than 20% frequency were not included for the alignment and analysis in the study.

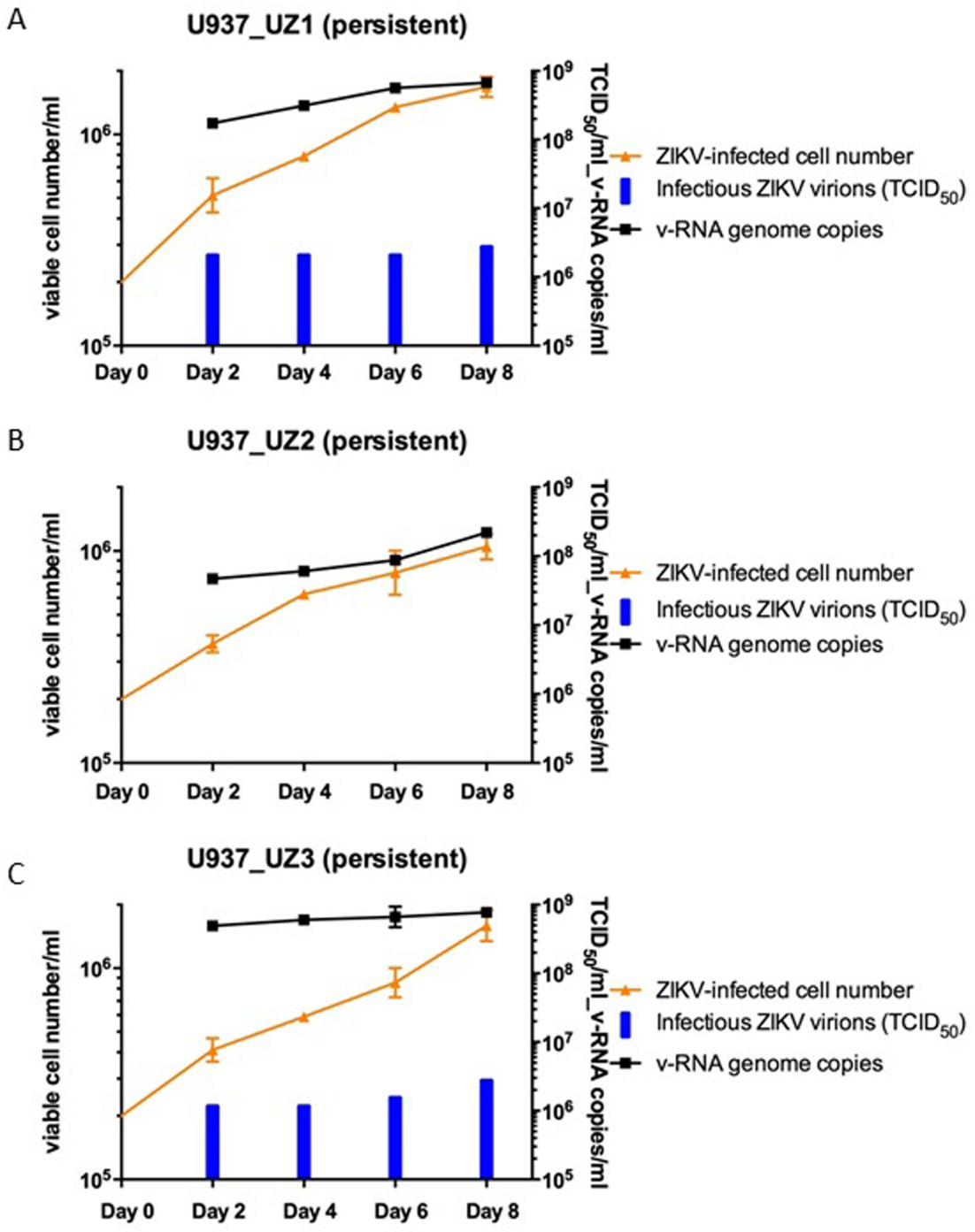

Fig 7. Cell growth, productions of ZIKV RNA genomes and infectious virions in cultures of the 3 continuous U937 cell lines established by further passing more than 2 months of the viable cells recovered from U937 cell cultures infected by the 3 persistent ZIKVs UZ1, UZ2 and UZ3. Cells in the persistently ZIKV-infected cultures (A) U937_UZ1 (persistent), (B) U937_UZ2 (persistent) and (C) U937_UZ3 (persistent) were harvested by centrifugation and re-suspended in fresh culture media every 2 days. The amounts of ZIKV RNA genomes and infectious virions produced into supernatants of the cultures in 2 days were quantified by qPCR and titrated by $TCID_{50}$ assay against Vero cells.

https://doi.org/10.1371/journal.pone.0203331.g007

Tables 3 and 4 summarize the ZIKV genomic sequencing results showing those variations or mutations with associated amino acid changes.

Table 3. The summary of the ZIKV RNA genomic variants identified in the inoculum prototype MR 766 ZIKV and ZIKVs produced by the acutely and persistently-infected U937 cells on the structure protein genes in comparison with the reported MR766 reference genomic sequence [22].

	Virus ID	Culture Supernatant	Position	115*	138*	338	641	767	780	841	879	1061	1116	1132	1139	1313	1368	1387	1395	1428
			Type	Del	Ins	SNV	SNV	SNV	SNV	SNV	SNV	SNV	SNV	SNV	SNV	SNV	SNV	SNV	SNV	SNV
			Reference	C	-	A	G	T	G	C	C	G	C	C	G	T	T	T	T	T
			Variant	-	T	G	A	C	T	T	T	A	T	A	A	A	A	C	G	A
1	MR 766 stock from BEI	MR 766 ZIKV/Vero-BEI	Variation associated with amino acid changes	Glu6fs, E6K, E7K, I8K, R9S, R10G, I11G	Arg12fs, R12F		D179N, 0.130			–, **0.217**								–, 0.550		
2	Inoculum Prototype MR 766 ZIKV	MR 766 ZIKV/Vero cells culture					D179N, 0.238			–, **0.264**								–, 0.528		
3	MR 766-U937-day 4	U937-MR 766_1 -4d culture					D179N, 0.185			–, **0.305**								–, 0.494		
4	MR 766-U937 -day 14	U937-MR 766_1 -14d culture					D179N, 0.727			–, **0.200**								–, 0.790		
5	UZ1-3m	U937_1-ZIKV -3m culture								– , **1.000**			T337M, 0.966						M430R, 0.971	
6	UZ1-4m	U937_1-ZIKV -4m culture											T337M, 0.844						M430R, 0.884	
7	UZ1-5m	U937_1-ZIKV -5m culture											T337M, 0.467						M430R, 0.467	
8	UZ1- U937-day 13	U937 infected with UZ1 (13d)											T337M, 1.000						M430R, 1.000	
9	UZ1.2-2m	U937_UZ1 (persistent culture)-2m				M78V, 0.484							T337M, 0.544				Q412R, 0.362		M430R, 0.494	
10	UZ1.2 -3m	U937_UZ1 (persistent culture)-3m				M78V, 0.334							T337M, 0.663				Q412R, 0.339		M430R, 0.073	
11	UZ2-4m	U937_2-ZIKV -4m culture													E345K, 1.000	L403M, 0.854				
12	UZ2- U937 -day 13	U937 infected with UZ2 (13d)													E345K, 0.882	L403M, 0.732				
13	UZ2.2-2m	U937_UZ2 (persistent culture)-2m						S221P, 0.429			A258V, 0.450			N342K, 0.512	E345K, 1.000					
14	UZ2.2-3m	U937_UZ2 (persistent culture)-3m						S221P, 0.609			A258V, 0.611			N342K, 0.472	E345K, 1.000					
15	UZ3-5.5m	U937_3-ZIKV -5.5m culture							R225M, 0.222			G319S, 0.333								M441K, 0.556
16	UZ3 - U937 -day 15	U937 infected with UZ3 (15d)							R225M, 0.674			G319S, 0.348								M441K, 0.619
17	UZ3.2-2.5m	U937_UZ3 (persistent culture)-2.5m							R225M, 1.000											M441K, 1.000
18	UZ3.2-4.5m	U937_UZ3 (persistent culture)-4.5m							R225M, 1.000											M441K, 1.000
Encoded Proteins			Mature peptide	Anchored capsid protein C			Membrane glycoprotein precursor M			Membrane glycoprotein M										
			nt sequence range	107-418; 107-472			473-751; 473-976			752-976										
			AA range	1-104; 1-122			123-215; 123-290			215-290										

Note: The coordination of the variants is corresponding to the reference genome sequence of the ZIKV MR 766 Uganda prototype retrieved from GenBank (Accession number NC_012532).

SNV stands for single nucleotide variation.

*: Single nucleotide insertion (Ins)/ deletion (Del) caused frameshift (fs). Light gray shadings: variants found in the inoculum prototype MR 766 ZIKV genome, which were different from the reference genome NC_012532.

The variations from the same set of experiment have identical background color. Empty cells indicate the absence of the variants on the corresponding positions; the number along with the amino acid change is its variation ratio found in the sample, the amino acid changes with variation ratio >0.99 were not labeled.

The synonymous nucleotide variant is indicated using a dash mark followed by its variation ratio. The three rows on the bottom indicate the spans of the encoded proteins on the viral polypeptide and which's corresponding positions of the viral RNA genome.

https://doi.org/10.1371/journal.pone.0203331.t003

Table 3. (Continued)

1451	1460	1466-1467	1492	1619	1646	1652	1788	1790	1812	1904	1913	1913	2120	2165	2316	2328
SNV	SNV	SNV	SNV	SNV	SNV	SNV	SNV	SNV	SNV	SNV	SNV	SNV	SNV	SNV	SNV	SNV
G	A	GA	G	C	G	G	C	G	G	T	G	G	T	C	C	C
A	G	TC	A	T	T	T	T	A	A	C	C	T	C	T	T	T
D449N			–, 0.067						**R596K**					**H687Y, 0.253**		S741L, 0.447
			–, 0.159											**H687Y, 0.268**		S741L, 0.282
			–, 0.132											**H687Y, 0.314**		S741L, 0.323
			–, 0.400											**H687Y, 0.350**		
											V603L, 0.953			**H687Y**		
											V603L, 0.878					
											V603L, 0.557					
											V603L, 1.000					
											V603L, 0.352	V603F, 0.625			A737V, 0.423	
											V603L, 0.063	V603F, 0.935			A737V, 0.311	
		E454 S, 0.838		H505Y, 0.842	G541W, 0.850		A561V, 0.770			F600L, 0.835						
		E454 S, 0.615		H505Y, 1.000	G541W, 0.989		A561V, 0.971			F600L, 1.000						
				H505Y, 0.486	G541W, 0.421		A561V, 0.371			F600L, 0.546						
				H505Y, 0.435	G541W, 0.422		A561V, 0.476			F600L, 0.433						
	K452E, 0.571					D516Y, 0.429		E562K, 0.517					T672H, 0.286			
	K452E, 0.366					D516Y, 0.275		E562K, 0.710					T672H, 0.327			
								E562K, 1.000								
								E562K, 1.000								
Envelope protein E																
977-2476																
291-790																

Table 4. The summary of the ZIKV RNA genomic variants identified in the inoculum prototype MR 766 ZIKV and ZIKVs produced by the acutely and persistently-infected U937 cells on the non-structure protein genes in comparison with the reported MR766 reference genomic sequence [22].

	Virus ID	Culture Supernatant	Position	2841	2511	2739	3650	3869	4257	4325	4822	5302	5444	6297	6507	6549	6569	6612	6659	6868
			Type	SNV	SNV	SNV	SNV	SNV	SNV	SNV	SNV	SNV	SNV	SNV	SNV	SNV	SNV	SNV	SNV	SNV
			Reference	A	A	T	G	C	C	A	G	G	A	C	A	G	C	C	T	G
			Variant	G	G	C	T	T	T	G	A	T	T	T	G	A	T	T	C	A
1	MR 766 stock from BEI	MR 766 ZIKV/Vero-BEI	Variation associated with amino acid changes					L1255F, 0.089			–, 0.090		N1780Y							
2	Inoculum Prototype MR 766 ZIKV	MR 766 ZIKV/Vero cells culture						L1255F, 0.100			–, 0.164									
3	MR 766-U937-day 4	U937-MR 766_1 -4d culture						L1255F, 0.101			–, 0.139									
4	MR 766-U937 -day 14	U937-MR 766_1 -14d culture									–, 0.400									
5	UZ1-3m	U937_1-ZIKV - 3m culture													E2134G, 0.580					
6	UZ1-4m	U937_1-ZIKV - 4m culture													E2134G, 0.720					
7	UZ1-5m	U937_1-ZIKV - 5m culture													E2134G, 0.692					
8	UZ1- U937 -day 13	U937 infected with UZ1 (13d)													E2134G,1.000					
9	UZ1.2-2m	U937_UZ1 (persistent culture)-2m								I1407V, 0.187					E2134G,0.897					
10	UZ1.2 -3m	U937_UZ1 (persistent culture)-3m								I1407V, 0.591					E2134G, 0.621			T2169I, 0.316		
11	UZ2-4m	U937_2-ZIKV - 4m culture							A1384V, 0.844					T2064I, 0.825		R2148Q, 0.800			F2185L, 0.580	
12	UZ2-U937 -day 13	U937 infected with UZ2 (13d)														R2148Q, 0.909			F2185L, 0.941	
13	UZ2.2-2m	U937_UZ2 (persistent culture)-2m													E2134G, 0.655		P2155S, 0.650		F2185L, 0.471	
14	UZ2.2-3m	U937_UZ2 (persistent culture)-3m			E802G, 0.594	V878A, 0.690									E2134G, 0.467		P2155S, 0.480		F2185L, 0.500	
15	UZ3-5.5m	U937_3-ZIKV - 5.5m culture										E1732D, 0.400			E2134G, 0.858					M2254I, 0.333
16	UZ3 - U937-day 15	U937 infected with UZ3 (15d)													E2134G, 0.753					M2254I, 0.753
17	UZ3.2-2.5m	U937_UZ3 (persistent culture)-2.5m		Y912C, 0.364			V1182L, 0.714								E2134G, 1.000					M2254I, 1.000
18	UZ3.2-4.5m	U937_UZ3 (persistent culture)-4.5m		Y912C, 0.750			V1182L, 0.286								E2134G, 1.000					M2254I, 1.000
	Encoded Proteins		Mature peptide	NS1			NS2A		NS2B		NS3				NS4A					Protein 2K
			nt sequence range	2477-3532			3533-4210		4211-4600		4601-6451				6452-6832					6833-6901
			AA range	791-1142			1143-1368		1369-1498		1499-2115				2116-2242					2243-2265

Note: The coordination of the variants is corresponding to the reference genome sequence of the ZIKV MR 766 Uganda prototype retrieved from GenBank (Accession number NC_012532).

SNV stands for single nucleotide variation.

*: Single nucleotide insertion (Ins)/ deletion (Del) caused frameshift (fs). Light gray shadings: variants found in the inoculum prototype MR 766 ZIKV genome, which were different from the reference genome NC_012532.

The variations from the same set of experiment have identical background color. Empty cells indicate the absence of the variants on the corresponding positions; the number along with the amino acid change is its variation ratio found in the sample, the amino acid changes with variation ratio >0.99 were not labeled.

The synonymous nucleotide variant is indicated using a dash mark followed by its variation ratio. The three rows on the bottom indicate the spans of the encoded proteins on the viral polypeptide and which's corresponding positions of the viral RNA genome.

https://doi.org/10.1371/journal.pone.0203331.t004

Table 4. (continued)

7157*	7160	7166*	7370	7519	7526	7563	7782	7815	7838	7851	7874	8030	8289	8845	8856	10126	10331	10698
Ins	SNV	Del	SNV	SNV	SNV	SNV	SNV	SNV	SNV	SNV	SNV	SNV	SNV	SNV	SNV	SNV	SNV	Ins
-	A	G	A	G	G	C	C	C	A	A	T	C	G	A	T	C	T	-
T	G	-	G	A	A	T	T	T	C	T	C	T	C	G	C	T	C	C
Met2353fs, M2352Y, H2353A,		Try2354fs, G2354W		–, 0.558					I2578L	E2582V			C2728S	–, 0.144		–, 0.568	–	–
				–, 0.550										–, 0.268		–, 0.568		
				–, 0.741										–, 0.229		–, 0.548		
				–, 0.833										–, 0.364		–, 0.563		
							A2559V, 0.207											
							A2559V, 0.600											
	Y2352C, 0.819		I2422V, 0.818															
	Y2352C, 0.745		I2422V, 0.767															
								A2570V, 0.438			Y2590H, 0.478							
						T2486I, 0.333		A2570V, 0.575			Y2590H, 0.564	L2642F, 0.450			I2917T, 0.560			
					G2474S, 0.400													
NS4B							NS5											3'UTR
6902-7654							7655-10363											10367-10794
2266-2516							2517-3419											

The previously reported prototype strain MR 766 ZIKV reference genomic sequence [22] with its nucleotide positions was used as the coordination in our comparative ZIKV genomic study. In comparison with the reference ZIKV genome sequence, the BEI-derived prototype strain MR 766 ZIKV and the inoculum MR 766 ZIKV strain propagated in Vero cells (MR 766/Vero) in our study had a deletion at position 115 and an insertion at position 138. These two close frameshifts resulted in a total 7 amino acid changes in this specific region of capsid protein C. In addition, the BEI-derived inoculum MR 766/Vero strain had 2 nucleotide mutations that occurred at positions 1451 and 1812 in the envelop protein E gene, and one mutation occurred at position 5444 in the NS3 gene. Moreover, a single nucleotide insertion and deletion caused frameshifts at positions 7157 and 7166 of the NS4B gene, and 3 mutations occurred at positions 7838, 7851 and 8289 in the NS5 gene. All 10 variations or mutations identified in the respective genes would result in amino acid changes. There was also one nucleotide insertion at position 10698 in the 3' end untranslated region (3'UTR). The variations identified at all these positions in the BEI-derived ZIKV prototype strain MR 766 were highly stable. They were consistently conserved in all the genomes of ZIKVs propagated in the cultures of Vero cells or produced in the cultures of U937 cells following both acute and persistent ZIKV infections (Tables 3 and 4). Remarkably, very few sequence heterogeneities were found at these positions among the raw reads generated using genome sequencing of all the ZIKV samples examined in this study.

Comparing genome sequences of ZIKVs produced by U937 cells after establishing the 1st and the 2nd rounds of persistent ZIKV infection with that of the inoculum prototype MR 766 ZIKV strain

Genomic sequencing studies of the BEI prototype ZIKV MR 766 viral stock and the inoculum MR 766/Vero revealed significant percentages of sequence reads with heterogeneity at positions 641, 841, 1387, 1492, 2165, 2328, 3869, 4822, 7519, 8845, 10126 (Tables 3 and 4, samples #1 and #2). Sequence heterogeneity at these positions continued to be present in the genomes of ZIKVs produced in the U937 cells cultures infected by the infectious viral stock inoculum MR 766/Vero in the early phase (1–2 weeks, samples # 3 and 4). However, heterogeneity of sequence reads disappeared completely at all these positions in the genomes of all 3 persistent ZIKVs (UZ1, UZ2 and UZ3, samples # 5–7, 11 and 15) produced by the U937 cells after establishment of ZIKV persistence in culture. The sequence heterogeneity continued to be absent at all these positions in the genomes of the 2nd generation persistent ZIKVs (UZ1.2, UZ2.2 and UZ3.2, samples # 9, 10, 13, 14, 17 and 18), despite the appearance of new sequence variations and heterogeneity at different gene positions (Tables 3 and 4).

Genomic analysis revealed that few new variations or mutations would be seen in the genomes of ZIKVs produced in U937 cell cultures following infections with either the inoculum prototype strain MR 766 ZIKV or the 3 persistent ZIKVs in the first 1–2 weeks (early phase, samples # 3, 4, 8, 12 and 16). However, in comparison with the genome sequence of the inoculum prototype strain MR 766 ZIKV, genomic analysis revealed 3 clearly different sets (color coded in Tables 3 and 4) of new variations or mutations with associated amino acid changes in the respective genomes of persistent ZIKVs, UZ1 (green), UZ2 (blue) and UZ3 (red) produced by the 3 continuous U937 cell lines after they established ZIKV persistence. These prominent new mutations occurred at distinct positions in the membrane glycoprotein M gene, envelope protein E gene and different NS genes of the 3 genomes of persistent ZIKVs, UZ1, UZ2 and UZ3 (Tables 3 and 4). Specifically, a set of mutations at positions 1116, 1395 and 1913 of envelop E gene as well as 6507 of NS4A gene was found in the genome of persistent ZIKV UZ1. A separate set of mutations at positions 1139, 1619, 1646, 1788 and 1904 of envelope E gene, as well as 6659 of NS4A gene was found in the genome of persistent ZIKV

UZ2. A third set of characteristic mutations at positions 1428 and 1790 of envelope E gene as well as 6507 of NS4A gene were found in the genome of persistent ZIKV UZ3. In addition, UZ3 had mutations at positions 780 of membrane glycoprotein M gene and 6868 of protein 2K gene. These mutations developed in genomes of the established persistent ZIKVs appeared to be rather stable. Our study showed that they persisted in the genomes of ZIKVs (UZ1-3m, UZ1-4m and UZ1-5m) produced by persistently ZIKV-infected culture U937_1 ZIKV passed weekly in cultures for 3 to 5 months (Table 3, samples 5–7).

Comparative ZIKV genomics showed that many of these mutations found in the 3 respective genomes of the 1st generation persistent ZIKVs continued to be present in the respective genomes of the 2nd generation persistent ZIKVs (UZ1.2, UZ2.2 and UZ3.2) produced by U937 cells that established a new round of ZIKV persistence following infections of the 1st generation of persistent ZIKVs UZ1, UZ2 and UZ3 in culture (Tables 3 and 4). However, some of the mutations disappeared and new mutations appeared. Amino acid changes not found in the genomes of the 1st generation of persistent ZIKVs UZ1, UZ2 and UZ3 were seen at some positions of Envelop E gene and NS genes in the genomes of the 2nd generation of persistent ZIKVs UZ1.2, UZ2.2 and UZ3.2. More nucleotide variations or mutations with associated amino acid changes could be seen in the genomes of persistent ZIKVs produced by the persistently ZIKV-infected culture U937_UZ1, U937_UZ2 passed weekly in cultures for a longer period (Tables 3 and 4).

Discussion

We examined human blood cell lines with different differentiation properties for possibly supporting continued propagation of ZIKV and developing ZIKV persistence. Consistent with the finding of a previous study [23], we found that the prototype ZIKV MR 766 strain infected human histiocytic lymphoma-originated U937 cells with very low efficiency and produced no detectable CPE changes with cytolytic necrosis in the ZIKV-infected cultures (Fig 2). However, our study revealed that supporting continuous growth of viable U937 cells in the cultures with low grade ZIKV infection would consistently lead to persistently ZIKV-infected U937 cell lines expressing ZIKV-specific antigens (Fig 3) and constantly producing both ZIKV RNA genomes and infectious virions (Fig 5). An additional study involving human cells of different developmental characteristics to infection using different ZIKV strains will be reported separately. Our preliminary results were in general consistent with those of other reports that an African ZIKV isolate (MR 766 strain) is more infectious and cytopathogenic than other isolates circulating in the Americas [24, 25] in the context of experimental infections involving various human host cells.

There were dynamic interplays between the ZIKVs and the infected human host cells in the intricate process of establishing viral persistence. However, the nature of viral population selection and host cell adaptation might be very different between the 2 respective rounds of establishing ZIKV persistence in U937 cells described in our study. Since the inoculum prototype strain MR 766 ZIKV could only infect and propagate in U937 cells at a very low rate, the slow kinetics of ZIKV infection may have resulted in the activation of various antiviral mechanisms in the U937 cells. This is consistent with the finding that none of the U937 cells in the three MR 766-infected cultures (Fig 2) had CPE changes and underwent cytolytic necrosis. In the prolonged process of establishing the 1st round of viral persistence in U937 cells, the specific groups or clones of ZIKVs with genetic variations or mutations in the key genes that enabled the viruses to effectively infect and propagate in the U937 cells, which had likely activated cellular antiviral mechanisms, were being selectively enriched from the heterogeneous population of the inoculum prototype strain MR 766 ZIKV. Interestingly, the 3 independently established persistent ZIKVs were composed of 3 highly selected "groups" or "clones" of ZIKV

carrying 3 distinct sets of mutations that were not found in the genome of the inoculum prototype strain MR 766 ZIKV. The pressure for selecting the ZIKV clones carrying a special set or combination of mutations would likely be needed to maintain the viral persistence in these U937 cell lines. The mutations that occurred were stably maintained in the ZIKVs produced by the persistently ZIKV-infected U937 cell lines passed weekly in culture for months (Tables 3 and 4), showing that the genetic changes introduced are essential for survival of the virus.

In the process of establishing the 2nd round of persistently ZIKV-infected U937 cell lines, fresh U937 cells were infected with the 3-established persistent ZIKVs UZ1, UZ2 and UZ3 that propagated effectively in U937 cells that had their antiviral mechanisms activated. Thus, large numbers of naïve U937 cells in the cultures infected by the 3 persistent ZIKVs quickly became IFA-positive for ZIKV antigen, developed prominent CPE changes and underwent cytolytic necrosis (Fig 5). The selection pressure in establishing the 2nd round of ZIKV persistence in cultures of U937 cells was mainly on selecting the special members or subpopulations of U937 cells that could sustain and adapt to growth in the cultures with active infections of ZIKVs. The process was no longer selecting the unique clones of ZIKVs with the specific biological properties. Thus, the 2nd generation persistent ZIKVs, UZ1.2, UZ2.2 and UZ3.2 produced by the 3 continuous U937 cell lines that established viral persistence following infections of the 1st generation of persistent ZIKVs, UZ1, UZ2 and UZ3 (Fig 1) retained many of the genetic mutations of the respective persistent ZIKVs (Tables 3 and 4). Not surprisingly, they also shared very similar properties in cell infectivity or pathogenicity of the respective 1st generation of persistent ZIKVs. However, both losing and gaining mutations at new genomic sites could also be seen in the genomes of the 2nd generation persistent ZIKVs UZ1.2, UZ2.2 and UZ3.2, especially when the 3 persistently ZIKV-infected U937 cell lines U937_UZ1, U937_UZ2 and U937_UZ3 were being passed in culture for longer periods of time (Tables 3 and 4).

The nucleotide variations or mutations identified in the genomes of the persistent ZIKVs UZ1, UZ2 and UZ3 resulted in specific amino acid changes at different positions of the key viral envelope protein E gene and NS4A genes (Tables 3 and 4). UZ2 had mutations at positions 7160 and 7370 of NS4B gene. UZ3 also had a mutation at position 780 of the membrane glycoprotein M gene and a mutation at position 6868 of the protein 2K gene between NS4A and NS4B genes. Each mutation or sets of mutations could be playing a vital role in the establishment and maintenance of ZIKV persistence in U937 cells. In this context, it is important to note that a single nucleotide variation at position 2165 of the envelop protein E gene, presenting with only low frequency in the inoculum MR 766 ZIKV genome, was shared without any sequence heterogeneity by all the genomes of persistent ZIKVs produced by U937 cell lines that emerged in both rounds of ZIKV persistence (Tablea 3 and 4). The mutation at this position could be highly critical in both developing and maintaining virus persistence in the ZIKV-infected human U937 cell lines. Both restricted expression and mutations of Flavivirus envelop E protein were reported previously to play a significant role in developing persistence of various Flaviviruses [26–29]. Mutations in the NS genes were also thought to be associated with viral persistence in WNV [30]. Other than playing a significant role in establishment and/or maintenance of viral persistence in the infected host cells, each of these identified mutations, individually or in various combinations could also play a prominent role in affecting the persistent ZIKVs' specificity in cell infectivity and pathogenicity. The mutations occurred in these genes were reported to be associated with cell infectivity and/or pathogenicity of ZIKV and WNV [31–36]. The biological significance of these mutations identified in the genomes of persistent ZIKVs warrants further studies.

More than 80 percent of natural ZIKV infections are asymptomatic low-grade infections and ZIKV can persist in the infected individuals for a prolonged period. Our *in-vitro* study of ZIKV persistence may have important clinical implications and further our understanding of

ZIKV evolution. A recent report [37] indicating that monocytes appeared to be the main targets of Zika virus infection in human PBMCs. Studying molecular mechanisms by which ZIKV establishes persistence in U937 cells of human monocytic/histiocytic origin should have high physiological and clinical relevance. The study showed that both viral and cellular mechanism played a role in the development of ZIKV persistence in U937 cells. One process involved selection of unique ZIKV clones with mutations in key viral genes enabling the viruses to continuously infect and proliferate in the human blood cells in which anti-viral mechanisms were activated. The other process involved selection of special human blood cells with adaptive metabolic functions enabling the cells to continuously grow without undergoing apoptosis or cytolysis, despite active propagation of ZIKVs. The persistent ZIKVs produced by the human U937 cells after independently developing viral persistence each time had properties not only distinct from the original ZIKV, but also among themselves in the specificity of cell infection and pathogenicity. The establishment of persistently ZIKV-infected human cell lines in our study may have the following implications. **(1)** They may facilitate future studies to determine molecular and biological bases of viral persistence in human cells. The gene expression profiles of human cells with persistent ZIKV infections can be analyzed in detail to explore the critical pathways that might accommodate or confer viral persistence. **(2)** The "permanent" human cell lines continuously producing ZIKV in culture may serve as a useful tool or platform for rapid screening of drugs or biologics as potential anti-viral therapeutics. **(3)** They may provide a useful model to evaluate various pathogen reduction methods or protocols developed to improve blood and tissue safety. **(4)** The persistently ZIKV-producing human cell lines may also be useful for vaccine development against ZIKV outbreaks.

Materials and methods

Virus and cells

Zika virus (ZIKV), MR 766 strain (NR-50065) and Genomic RNA from Zika virus, MR 766 (NR-50085) were obtained from BEI Resources, NIAID/NIH. Human cell lines CCRF-SB (B lymphoblast, ATCC CCL-120), CCRF-CEM (T lymphoblast, ATCC CRM-CCL-119), CCRF-HSB2 (T lymphoblast, ATCC CCL-120.1), K562 (lymphoblast, ATCC CCL243), U937 (histiocytic lymphoma, ATCC CRL-1593.2), THP-1 (monocyte, ATCC TIB202), HL-60 (promyeloblast, ATCC CCL240) and KG-1 (lymphoblast, ATCC CRL-8031) as well as Vero cells (African green monkey kidney cells, ATCC CCL-81) were obtained from ATCC. RPMI-8392 (B cell line 8392, GM03638) and RPMI-8402 (T cell line 8402, GM03639) were obtained from NIGMS Human Genetic Mutant Cell Repository. Molt-3 (human T lymphoblast) was obtained from Biotech Research Labs, Rockville MD. The human B cell line K2267-Mi was previously established and characterized in our laboratory [38]. EBV-positive human lymphoblastoid B-cell lines 824–00 was developed from spontaneous immortalization of healthy blood donor PBMC and 4695EB was established from human B cells immortalized by EBV strain B95-8 transformation in our laboratory. Unless specified otherwise, cell cultures were grown in RPMI 1640 medium supplemented with 10% fetal bovine serum (FBS) and 1% penicillin-streptomycin solution at 37˚C and 5% CO_2.

Propagation of the ZIKV MR 766 working stock

A T75 culture flask with 90% confluent Vero cells kept in 10 ml of RPMI 1640 medium containing 2% FBS (R2 medium) was infected with ZIKV MR 766 obtained from BEI Resources at multiplicity of infection (MOI) of 0.1–0.01 according to the package description. The ZIKV-infected Vero cell culture was incubated in a CO2 incubator at 37˚C and monitored daily for the appearance of viral CPE. The culture supernatant was harvested by centrifugation, when

~80% of cells detached from the culture surface of the flask after developing CPE. The culture supernatant was filtered to remove cell debris, aliquoted, tittered and stored at -80˚C as the ZIKV working stock to be used in the subsequent experiments.

Infection of human hematopoietic cell lines with Zika virus

About 2×10^6 cells were harvested from an actively growing suspension cell culture by centrifugation in a 15-ml tube. Cells were washed once with R2 medium and collected by centrifugation. The washed cells were suspended in 0.3 ml of R2 medium containing 4×1060020030p.f.u. of ZIKV MR 766, and incubated at 37˚C for 2 hours with frequent shaking to adjust the virus inoculum to ~2 MOI (if not otherwise specified). After incubation, cells were washed with fresh R2 medium for 3 times, and cultured in 10 ml of RPMI 1640 medium supplemented with 10% FBS in a T-25 culture flask kept at 37˚C in 5% CO_2 incubator. The starting cell concentration in culture was normally adjusted to $1–2\times10^5$ cells/ml. At the designated time points, 0.5 ml of each suspension cell culture was sampled to perform viable cell count and IFA study to identify and quantify Flavivirus group antigen-positive cells. Culture supernatants were stored at -80˚C for quantitative measurements of infectious ZIKV virions by endpoint dilution assay as well as v-RNA genome copies by real-time reverse transcription-PCR.

Endpoint dilution assay ($TCID_{50}$)

Infectious titer was measured as the 50% tissue culture infective dose ($TCID_{50}$), using Vero cells. Exponentially growing Vero cells were seeded in a 96-well culture plate at 2×10^4 cells/well in RPMI 1640 medium containing 10% FBS one day before performing the assay. Aliquots of supernatants collected previously from ZIKV-infected cell cultures at the designated time points were 10-fold serially diluted in R2 medium. In the assay, the culture medium of the prepared 96-well plates of Vero cells was aspirated and 20 μl of serially diluted culture supernatant of ZIKV working stock was added into each well. Eight wells were inoculated for each dilution of the culture supernatant tested. After incubating the plates at 37˚C for 2 hours for viral absorption, 150 μl fresh R2 medium were added into each well. The plates were incubated in a CO2 incubator at 37˚C and followed for 4 to 6 days. At the end of assay, the numbers of culture wells showing clear viral CPE was recorded. The $TCID_{50}$ titer was calculated based on the method described by Hierholzer & Kilington in the first edition of the Virology Methods Manual.

Immunofluorescence assay

To prepare cell samples for immunofluorescence assay (IFA), 0.5 ml of the cell suspension was harvested from a cell culture and centrifuged at 1000 rpm for 10 min in a microfuge tube. The cell pellet was washed with 1ml of phosphate buffered saline (PBS). After centrifugation, the cell pellet was re-suspended in 50 μl of PBS and 10–20 μl of cell suspension was dotted on a microscopic slide. The cell slides were air-dried and then fixed with mixture of methanol: acetone (1:1) for 5 min at room temperature. To detect the presence of ZIKV antigenic proteins in cells, Anti-Flavivirus Group antigen monoclonal antibody (Clone D1-4G2-4-15, BEI Resources) was used as the primary antibody of IFA to detect cells that were positive for producing ZIKV antigen. Cell dots were blocked for 30 min with a blocking solution (KPL, Gaithersburg MD, USA), and 1% bovine serum albumin (BSA) in PBS containing 100 μg/ml of human immunoglobulin. Cell smears on the slides were then incubated with primary antibody (1:300 dilutions in 1% BSA-PBS) at room temperature for 30min in a humidified chamber. After washing with PBS, 3 times, the cell smears were incubated with a secondary antibody, Alexa Fluor 488 conjugated goat-anti-mouse IgG (1:400) (Jackson ImmunoResearch Labs, PA) for

30min. The slide was washed with PBS, 3 times and then once with distilled water. The slides were air dried and mounted with glycerol-PBS mixture containing DAPI (4',6-diamidino-2-phenylindole, Sigma, Mo). The cell images were captured using an up-right immunofluorescent microscope with attached digital camera system (Olympus BX51).

Electron microscopy

For transmission electron microscopy (TEM), cell samples were centrifuged at 2000 rpm for 10 min in a microfuge tube, a small cell pellet was then fixed with 2.5% glutaraldehyde in 0.1M sodium cacodylate buffer pH7.4 at 4˚C for overnight and post-fixed with 1% OsO_4 in PBS. Samples were dehydrated in a series 50%, 70%, 95% of ethanol for 10 min each, 3 times in 100% ethanol for 10 min each, and 3 times in propylene oxide for 10 min each. The samples were then processed for infiltration of propylene with Epon12 overnight at RT and embedded in Epon12 epoxy resin at 60 ^{o}C in the oven for 48 hours. Ultrathin sections were cut by ultramicrotome, stained with uranyl acetate and lead citrate, and then examined with a Zeiss Libra 120 Plus transmission electron microscope. The electron micrographs were taken with a Gatan US1000XP digital camera.

Real-time one-step reverse transcription-quantitative PCR (RT-qPCR)

Quantification of v-RNA of ZIKV genome was performed by a real-time RT-PCR assay using ZIKV-specific primer sets. Total RNA of a culture supernatant was extracted from 140 μl of sample stored at -80˚C using QIAamp Viral RNA Mini Kit (Qiagen, Dusseldorf Germany), following the manufacturer's protocol. The v-RNA copy numbers in purified RNA were quantified using iTaq Universal SYBR Green One-Step Kit (Bio-Rad, CA USA) and Bio-Rad CFX96 system (Bio-Rad, CA USA). Each reaction mixture of one-step RT-qPCR contained 5 μl of purified RNA, 10 μl of iTaq universal SYBR Green reaction mix, 0.25 μl of iScript reverse transcriptase, 0.5 μl each of 10uM forward and reverse primer, and 4.25 μl of nuclease-free water, to a final volume of 20 μl. The RT-PCR was started from 50˚C reverse transcription step for 30 min and followed by PCR amplification with 95˚C pre-heat for 1 min and then 45 two-step thermocycles at 95˚C for 10 sec and 57˚C for 30 sec. The ZIKV-specific primer pair used in the RT-qPCR reaction was described previously [39]. The sequences of the forward and reverse primers are: 5′-CCTTGGATTCTTGAACGAGGA-3′ and 5′-AGAGCTTCATTCTCCAGATCAA-3′. The standard curve for estimating v-RNA copy number present in the tested sample was calculated by fitting the Ct value to a strand curve. The standard curve was generated by RT-PCR run against six RNA samples prepared from a10-fold serial dilution of the ZIKV MR 766 genomic RNA solution containing 1.1×10^{6} ZIKV RNA genome copies/μl provided by BEI.

Viral RNA preparation for viral genome sequencing

RNAs of viral particles were extracted from the cell culture supernatant. Culture supernatant, 50 ml, from acute or persistent infected cells was harvested. The supernatant was centrifuged at 2000g for 10 min, dispersed and passed through a 0.22 μm filter to further remove cell residuals. The supernatant was chilled on an ice-bath and 20 ml of 20% PEG (polyethylene glycol)-8000 solution (with 2.5M NaCl) was added into culture supernatant. The PEG-supernatant mixture was stored at 4˚C, overnight. The overnight chilled mixture was centrifuged at 3000g, 4˚C for 30 min. The supernatant was discarded and the precipitate was re-suspended in100 μl of PBS. Trizol Reagent, 300 μl, was added into the viral suspension to extract viral RNA using Direct-zol MiniPrep kit (Zymo Research, CA, USA), following the procedures provided by the manufacturer. The extracted RNA samples were quality checked and quantified by RNA pico chips of 2100 Bioanalyzer (Agilent, CA, USA).

RNA-Seq of viral genome

The RNAs from supernatants were used to generate libraries using Illumina TruSeq stranded total RNA sample prep kit, following the manufacturer's standard procedures. In brief, total RNA were fragmented in the presence of divalent ions at 94˚C for 8 minutes. Fragmented RNAs were reverse-transcribed into first-strand cDNAs, and then second-strand cDNAs. The double strand cDNAs were adenylated at the 3' ends, ligated to indexed sequencing adaptors, and amplified for 15 cycles. The cDNA Libraries were loaded in one MiSeq Nano Flow Cell using MiSeq Reagent Nano kit for a 100-cycle paired-end sequencing on the MiSeq sequencer (Illumina, San Diego, CA, USA).

Analysis of the viral genome variants

The fastq files generated from the Illumina MiSeq sequencer were used for viral genome variant analysis. All the sequence analyses were performed by the software package CLC Genomics Workbench version 9.5.3. The raw reads were trimmed to remove the regions with more than two ambiguous bases, and the regions having 5% of the bases with quality score lower than 20. The trimmed reads were mapped to the reference sequence of the ZIKV MR 766 Uganda prototype (GenBank Accession number: NC_012532) with the mapping parameter: match score = 1, Mismatch cost = 2, insertion cost = 3, deletion cost = 3, mapped length fraction>0.5, and similarity fraction>0.8. The local realignment was applied to realign the unaligned ends from the reads mapping. The aligned reads tracks from the local realignment were used for Low Frequency Variant Detection with the parameter: Ploidy = 1, required variant probability = 80%, the minimum coverage = 5, minimum reads count = 2, minimum frequency = 1%. The reads mapping BAM file of each analyzed sample listed on Tables 3 and 4 can be downloaded from Dryad repository, doi:10.5061/dryad.7r7812c.

Supporting information

S1 Fig. Electron micrographs of persistently ZIKV-infected U937_ZIKV-1 cell line (A) and persistently ZIKV-infected U937_ZIKV-2 cell line (B) with size bars. Insert Boxes: Electron-dense virus-like particles (red arrows) in higher magnification. Yellow arrow head: Cell membrane. N: Nucleus. M: Mitochondria.
(TIF)

S2 Fig. Atypical CPE without cytolysis seen in the $TCID_{50}$ assay wells seeded with Vero cells and inoculated ($<10^1$ dilution) with low dilutions of supernatant from the U937_ZIKV-2 culture. A1 (100X) and A2 (400X): Vero cells seeded in the $TCID_{50}$ assay well inoculated with supernatant of the control U937 cell culture showed no CPE changes at day 3. Vero cells in the assay wells inoculated with the inoculum prototype MR 766 strain ZIKV and supernatant of the persistently ZIKV-infected U937_ZIKV-1 cell culture showed prominent CPE changes at day 3. **B1 (100X) and B2 (400X):** Vero cells seeded in the $TCID_{50}$ assay well inoculated with supernatant of the control U937 cell culture showed no CPE-associated cytolysis at day 5. Vero cells in the assay wells inoculated with the inoculum prototype MR 766 strain ZIKV and UZ1 from supernatant of the persistently ZIKV-infected U937_ZIKV-1 cell culture showed prominent CPE with extensive cytolysis and cell sloughing at day 5. Vero cells in the assay wells inoculated with UZ2 from supernatant of the persistently ZIKV-infected U937_ZIKV-2 cell culture had clusters of cells with atypical CPE changes at day 5. However, no cytolysis or cell sloughing was seen in the well (A1 and A2). Vero cells in these $TCID_{50}$ assay wells had no cytolysis or cell sloughing even at day 7 post inoculation of UZ2 from supernatant

of the persistently ZIKV-infected U937_ZIKV-2 cell culture (B1 and B2).
(TIF)

S3 Fig. Cell growth, numbers of cells IFA-positive for ZIKV antigen, productions of ZIKV RNA genomes and infectious virions in cultures of K562 cells infected with the 3 persistent ZIKVs UZ1(A), UZ2 (B) and UZ3 (C). The cultures of K562 cells (2×10^5 cells/ml) were infected with the 3 persistent ZIKVs (~10^7 copies of ZIKV v-RNA genome/ml) prepared from the culture supernatants of persistently ZIKV-infected U937 cell lines U937_1-ZIKV, U937_2-ZIKV and U937_3-ZIKV. Prominent CPE with extensive cytolysis and cell loss were seen in all the 3 cultures infected with the 3 persistent ZIKVs UZ1, UZ2 and UZ3. The amounts of ZIKV RNA genomes and infectious virions produced into supernatants of the ZIKV-infected cultures were quantified by qPCR and titrated by $TCID_{50}$ assay against Vero cells.
(TIF)

Acknowledgments

We thank Dr. Robert Aksamit and Dr. Jakob Reiser at the Center for Biologics Evaluation and Research, Food and Drug Administration (Silver Spring, Maryland) for reviewing and editing the manuscript for publication.

The following reagents, Genomic RNA from Zika virus MR 766, NR-50085, Monoclonal Anti-Flavivirus Group Antigen, Clone D1-4G2-4-15 (produced in vitro), NR-50327 and Zika Virus MR 766, NR-50065, were obtained through BEI Resources, NIAID, NIH, and Zika Virus MR 766, NR-50065 was as part of the WRCEVA program.

The viral RNA genome sequencing was supported by the Protein and Nucleic Acid Laboratory under Facility for Biotechnology Resources, Center for Biologics Evaluation and Research, Food and Drug Administration.

This project was supported in part by an appointment to the Research Fellowship Program at the Office of Tissue and Advanced Therapies/ Center for Biologics Evaluation and Research, U.S. Food and Drug Administration (FDA), administered by the Oak Ridge Institute for Science and Education through an interagency agreement between the U.S. Department of Energy and FDA.

Author Contributions

Conceptualization: Shien Tsai, Shyh-Ching Lo.

Data curation: Bingjie Li, Hsiao-Mei Liao, Hebing Liu, Shien Tsai, Shyh-Ching Lo.

Formal analysis: Hsiao-Mei Liao, Hebing Liu, Jing Zhang, Pei-Ju Chin, Yamei Gao.

Investigation: Bingjie Li, Hsiao-Mei Liao, Shien Tsai, Guo-Chiuan Hung.

Methodology: Bingjie Li, Hsiao-Mei Liao, Hebing Liu, Jing Zhang, Yamei Gao.

Supervision: Shyh-Ching Lo.

Writing – original draft: Shyh-Ching Lo.

Writing – review & editing: Shien Tsai, Pei-Ju Chin, Shyh-Ching Lo.

References

1. Heymann DL, Hodgson A, Sall AA, Freedman DO, Staples JE, Althabe F, et al. Zika virus and microcephaly: why is this situation a PHEIC? Lancet. 2016; 387(10020):719–21. https://doi.org/10.1016/S0140-6736(16)00320-2 PMID: 26876373.

2. Malone RW, Homan J, Callahan MV, Glasspool-Malone J, Damodaran L, Schneider Ade B, et al. Zika Virus: Medical Countermeasure Development Challenges. PLoS neglected tropical diseases. 2016; 10 (3):e0004530. https://doi.org/10.1371/journal.pntd.0004530 PMID: 26934531; PubMed Central PMCID: PMCPMC4774925.
3. Mlakar J, Korva M, Tul N, Popovic M, Poljsak-Prijatelj M, Mraz J, et al. Zika Virus Associated with Microcephaly. N Engl J Med. 2016; 374(10):951–8. https://doi.org/10.1056/NEJMoa1600651 PMID: 26862926.
4. Schuler-Faccini L, Ribeiro EM, Feitosa IM, Horovitz DD, Cavalcanti DP, Pessoa A, et al. Possible Association Between Zika Virus Infection and Microcephaly—Brazil, 2015. MMWR Morb Mortal Wkly Rep. 2016; 65(3):59–62. https://doi.org/10.15585/mmwr.mm6503e2 PMID: 26820244.
5. Bullard-Feibelman KM, Govero J, Zhu Z, Salazar V, Veselinovic M, Diamond MS, et al. The FDA-approved drug sofosbuvir inhibits Zika virus infection. Antiviral research. 2017; 137:134–40. Epub 2016/12/03. https://doi.org/10.1016/j.antiviral.2016.11.023 PMID: 27902933; PubMed Central PMCID: PMCPMC5182171.
6. Giersing BK, Vekemans J, Nava S, Kaslow DC, Moorthy V, Committee WHOPDfVA. Report from the World Health Organization's third Product Development for Vaccines Advisory Committee (PDVAC) meeting, Geneva, 8-10th June 2016. Vaccine. 2017. https://doi.org/10.1016/j.vaccine.2016.10.090 PMID: 28262332.
7. Burkhalter KL, Wiggins K, Burkett-Cadena N, Alto BW. Laboratory Evaluation of Commercially Available Platforms to Detect West Nile and Zika Viruses From Honey Cards. J Med Entomol. 2018. Epub 2018/02/21. https://doi.org/10.1093/jme/tjy005 PMID: 29462341.
8. Carossino M, Li Y, Lee PA, Tsai CF, Chou PH, Williams D, et al. Evaluation of a field-deployable reverse transcription-insulated isothermal PCR for rapid and sensitive on-site detection of Zika virus. BMC infectious diseases. 2017; 17(1):778. Epub 2017/12/21. https://doi.org/10.1186/s12879-017-2852-4 PMID: 29258444; PubMed Central PMCID: PMCPMC5735522.
9. Cairns DM, Boorgu D, Levin M, Kaplan DL. Niclosamide rescues microcephaly in a humanized in vivo model of Zika infection using human induced neural stem cells. Biol Open. 2018; 7(1). Epub 2018/01/31. https://doi.org/10.1242/bio.031807 PMID: 29378701.
10. Mesci P, Macia A, Moore SM, Shiryaev SA, Pinto A, Huang CT, et al. Blocking Zika virus vertical transmission. Sci Rep. 2018; 8(1):1218. Epub 2018/01/21. https://doi.org/10.1038/s41598-018-19526-4 PMID: 29352135; PubMed Central PMCID: PMCPMC5775359.
11. Gourinat AC, O'Connor O, Calvez E, Goarant C, Dupont-Rouzeyrol M. Detection of Zika virus in urine. Emerg Infect Dis. 2015; 21(1):84–6. https://doi.org/10.3201/eid2101.140894 PMID: 25530324; PubMed Central PMCID: PMC4285245.
12. Musso D, Roche C, Nhan TX, Robin E, Teissier A, Cao-Lormeau VM. Detection of Zika virus in saliva. J Clin Virol. 2015; 68:53–5. https://doi.org/10.1016/j.jcv.2015.04.021 PMID: 26071336.
13. Miner JJ, Sene A, Richner JM, Smith AM, Santeford A, Ban N, et al. Zika Virus Infection in Mice Causes Panuveitis with Shedding of Virus in Tears. Cell Rep. 2016; 16(12):3208–18. https://doi.org/10.1016/j.celrep.2016.08.079 PMID: 27612415; PubMed Central PMCID: PMC5040391.
14. Paz-Bailey G, Rosenberg ES, Doyle K, Munoz-Jordan J, Santiago GA, Klein L, et al. Persistence of Zika Virus in Body Fluids—Preliminary Report. N Engl J Med. 2017. https://doi.org/10.1056/NEJMoa1613108 PMID: 28195756.
15. Iwamoto M, Jernigan DB, Guasch A, Trepka MJ, Blackmore CG, Hellinger WC, et al. Transmission of West Nile virus from an organ donor to four transplant recipients. N Engl J Med. 2003; 348 (22):2196–203. https://doi.org/10.1056/NEJMoa022987 PMID: 12773646.
16. Centers for Disease C, Prevention. West Nile virus transmission via organ transplantation and blood transfusion—Louisiana, 2008. MMWR Morb Mortal Wkly Rep. 2009; 58(45):1263–7. PubMed PMID: 19940831.
17. Coffey LL, Pesavento PA, Keesler RI, Singapuri A, Watanabe J, Watanabe R, et al. Zika Virus Tissue and Blood Compartmentalization in Acute Infection of Rhesus Macaques. PloS one. 2017; 12(1): e0171148. https://doi.org/10.1371/journal.pone.0171148 PMID: 28141843; PubMed Central PMCID: PMCPMC5283740 employees does not alter our adherence to PLOS ONE policies on sharing data and materials.
18. Aid M, Abbink P, Larocca RA, Boyd M, Nityanandam R, Nanayakkara O, et al. Zika Virus Persistence in the Central Nervous System and Lymph Nodes of Rhesus Monkeys. Cell. 2017; 169(4):610–20 e14. https://doi.org/10.1016/j.cell.2017.04.008 PMID: 28457610.
19. Hirsch AJ, Smith JL, Haese NN, Broeckel RM, Parkins CJ, Kreklywich C, et al. Zika Virus infection of rhesus macaques leads to viral persistence in multiple tissues. PLoS Pathog. 2017; 13(3):e1006219. https://doi.org/10.1371/journal.ppat.1006219 PMID: 28278237; PubMed Central PMCID: PMCPMC5344528.

20. Jean Michel M, Catherine M, Christophe P, Sabine C-R, Pierre D, Guillaume M-B, et al. Zika Virus Infection and Prolonged Viremia in Whole-Blood Specimens. Emerging Infectious Disease journal. 2017; 23 (5). https://doi.org/10.1007/s00705-006-0903-z.

21. Ralph P, Moore MA, Nilsson K. Lysozyme synthesis by established human and murine histiocytic lymphoma cell lines. J Exp Med. 1976; 143(6):1528–33. PMID: 1083890; PubMed Central PMCID: PMC2190228.

22. Kuno G, Chang GJ. Full-length sequencing and genomic characterization of Bagaza, Kedougou, and Zika viruses. Arch Virol. 2007; 152(4):687–96. https://doi.org/10.1007/s00705-006-0903-z PMID: 17195954.

23. Chan JF, Yip CC, Tsang JO, Tee KM, Cai JP, Chik KK, et al. Differential cell line susceptibility to the emerging Zika virus: implications for disease pathogenesis, non-vector-borne human transmission and animal reservoirs. Emerg Microbes Infect. 2016; 5:e93. https://doi.org/10.1038/emi.2016.99 PMID: 27553173; PubMed Central PMCID: PMCPMC5034105.

24. Simonin Y, Loustalot F, Desmetz C, Foulongne V, Constant O, Fournier-Wirth C, et al. Zika Virus Strains Potentially Display Different Infectious Profiles in Human Neural Cells. EBioMedicine. 2016; 12:161–9. https://doi.org/10.1016/j.ebiom.2016.09.020 PMID: 27688094; PubMed Central PMCID: PMCPMC5078617.

25. Devhare P, Meyer K, Steele R, Ray RB, Ray R. Zika virus infection dysregulates human neural stem cell growth and inhibits differentiation into neuroprogenitor cells. Cell Death Dis. 2017; 8(10):e3106. Epub 2017/10/13. https://doi.org/10.1038/cddis.2017.517 PMID: 29022904; PubMed Central PMCID: PMCPMC5682681.

26. Feng G, Takegami T, Zhao G. Characterization and E protein expression of mutant strains during persistent infection of KN73 cells with Japanese encephalitis virus. Chin Med J (Engl). 2002; 115(9):1324–7. PubMed PMID: 12411104.

27. Ding X, Wu X, Duan T, Siirin M, Guzman H, Yang Z, et al. Nucleotide and amino acid changes in West Nile virus strains exhibiting renal tropism in hamsters. Am J Trop Med Hyg. 2005; 73(4):803–7. PubMed PMID: 16222029.

28. Farfan-Ale JA, Lorono-Pino MA, Garcia-Rejon JE, Hovav E, Powers AM, Lin M, et al. Detection of RNA from a novel West Nile-like virus and high prevalence of an insect-specific flavivirus in mosquitoes in the Yucatan Peninsula of Mexico. Am J Trop Med Hyg. 2009; 80(1):85–95. PubMed PMID: 19141845; PubMed Central PMCID: PMCPMC2663380.

29. Sanchez-Vargas I, Scott JC, Poole-Smith BK, Franz AW, Barbosa-Solomieu V, Wilusz J, et al. Dengue virus type 2 infections of Aedes aegypti are modulated by the mosquito's RNA interference pathway. PLoS Pathog. 2009; 5(2):e1000299. https://doi.org/10.1371/journal.ppat.1000299 PMID: 19214215; PubMed Central PMCID: PMCPMC2633610.

30. Saxena V, Xie G, Li B, Farris T, Welte T, Gong B, et al. A hamster-derived West Nile virus isolate induces persistent renal infection in mice. PLoS neglected tropical diseases. 2013; 7(6):e2275. https://doi.org/10.1371/journal.pntd.0002275 PMID: 23785537; PubMed Central PMCID: PMCPMC3681636.

31. Jun SR, Wassenaar TM, Wanchai V, Patumcharoenpol P, Nookaew I, Ussery DW. Suggested mechanisms for Zika virus causing microcephaly: what do the genomes tell us? BMC Bioinformatics. 2017; 18 (Suppl 14):471. Epub 2018/01/04. https://doi.org/10.1186/s12859-017-1894-3 PMID: 29297281; PubMed Central PMCID: PMCPMC5751795.

32. Yuan L, Huang XY, Liu ZY, Zhang F, Zhu XL, Yu JY, et al. A single mutation in the prM protein of Zika virus contributes to fetal microcephaly. Science (New York, NY). 2017; 358(6365):933–6. Epub 2017/10/04. https://doi.org/10.1126/science.aam7120 PMID: 28971967.

33. Liang Q, Luo Z, Zeng J, Chen W, Foo SS, Lee SA, et al. Zika Virus NS4A and NS4B Proteins Deregulate Akt-mTOR Signaling in Human Fetal Neural Stem Cells to Inhibit Neurogenesis and Induce Autophagy. Cell Stem Cell. 2016; 19(5):663–71. Epub 2016/08/16. https://doi.org/10.1016/j.stem.2016.07.019 PMID: 27524440; PubMed Central PMCID: PMCPMC5144538.

34. Campbell CL, Smith DR, Sanchez-Vargas I, Zhang B, Shi PY, Ebel GD. A positively selected mutation in the WNV 2K peptide confers resistance to superinfection exclusion in vivo. Virology. 2014;464–465:228–32. Epub 2014/08/12. https://doi.org/10.1016/j.virol.2014.07.009 PMID: 25104615; PubMed Central PMCID: PMCPMC4486337.

35. Roosendaal J, Westaway EG, Khromykh A, Mackenzie JM. Regulated cleavages at the West Nile virus NS4A-2K-NS4B junctions play a major role in rearranging cytoplasmic membranes and Golgi trafficking of the NS4A protein. J Virol. 2006; 80(9):4623–32. Epub 2006/04/14. https://doi.org/10.1128/JVI.80.9.4623-4632.2006 PMID: 16611922; PubMed Central PMCID: PMCPMC1472005.

36. Zou G, Puig-Basagoiti F, Zhang B, Qing M, Chen L, Pankiewicz KW, et al. A single-amino acid substitution in West Nile virus 2K peptide between NS4A and NS4B confers resistance to lycorine, a flavivirus

inhibitor. Virology. 2009; 384(1):242–52. Epub 2008/12/09. https://doi.org/10.1016/j.virol.2008.11.003 PMID: 19062063; PubMed Central PMCID: PMCPMC5388927.

37. Michlmayr D, Andrade P, Gonzalez K, Balmaseda A, Harris E. CD14(+)CD16(+) monocytes are the main target of Zika virus infection in peripheral blood mononuclear cells in a paediatric study in Nicaragua. Nat Microbiol. 2017; 2(11):1462–70. Epub 2017/10/04. https://doi.org/10.1038/s41564-017-0035-0 PMID: 28970482; PubMed Central PMCID: PMCPMC5997390.

38. Zhang S, Tsai S, Wu TT, Li B, Shih JW, Lo SC. Mycoplasma fermentans infection promotes immortalization of human peripheral blood mononuclear cells in culture. Blood. 2004; 104(13):4252–9. Epub 2004/08/28. https://doi.org/10.1182/blood-2004-04-1245 PMID: 15331449.

39. Balm MN, Lee CK, Lee HK, Chiu L, Koay ES, Tang JW. A diagnostic polymerase chain reaction assay for Zika virus. Journal of medical virology. 2012; 84(9):1501–5. https://doi.org/10.1002/jmv.23241 PMID: 22825831.